International Journal of Biological Macromolecules xxx (xxxx) xxx

Contents lists available at ScienceDirect

International Journal of Biological Macromolecules

journal homepage: www.elsevier.com/locate/ijbiomac

Core-sheath nanostructured chitosan-based nonwovens as a potential drug delivery system for periodontitis treatment

Danilo M. dos Santos [a,*], Paulo A.M. Chagas [a,b], Ilaiáli S. Leite [c], Natalia M. Inada [c], Sarah R. de Annunzio [d], Carla R. Fontana [d], Sérgio P. Campana-Filho [e], Daniel S. Correa [a,b,*]

[a] Nanotechnology National Laboratory for Agriculture (LNNA), Embrapa Instrumentação, 13560-970 São Carlos, SP, Brazil
[b] PPG-Biotec, Center for Exact Sciences and Technology, Federal University of São Carlos (UFSCar), 13565-905 São Carlos, SP, Brazil
[c] Sao Carlos Institute of Physics/University of São Paulo, PO Box 369, 13560-970 São Carlos, São Paulo, Brazil
[d] Department of Clinical Analysis, School of Pharmaceutical Sciences, São Paulo State University (UNESP), 14800-903 Araraquara, São Paulo, Brazil
[e] Sao Carlos Institute of Chemistry/University of São Paulo, Av. Trabalhador sao-carlense, 400, 13566-590 São Carlos, São Paulo, Brazil

ARTICLE INFO

Article history:
Received 11 June 2019
Received in revised form 14 August 2019
Accepted 16 September 2019
Available online xxxx

Keywords:
Chitosan
Coaxial electrospinning
Nanocarrier

ABSTRACT

Core-sheath nanofibers were successfully prepared *via* coaxial electrospinning by using chitosan with well-defined structural characteristics as the shell layer and poly (vinyl alcohol) (PVA) containing tetracycline hydrochloride (TH) as the core layer. The effects of the average degree of deacetylation ($\overline{DD}$) of chitosan and the post-electrospinning genipin crosslinking on physicochemical and biological properties of resulting nonwovens were evaluated. Defect-free and geometrically uniform nanofibers with diameters predominantly in the range of 100–300 nm were prepared, and transmission electron microscopy (TEM) revealed the core-sheath structures and its preservation after crosslinking. The mechanical properties, as well as the stability of nonwovens in aqueous medium, were greatly improved by genipin-crosslinking, which enabled a sustained release of TH over 14 days. Results also revealed that the release profile of TH in the presence of lysozyme was affected by the composition of the shell layer, as the TH release rate increases with decreasing of $\overline{DD}$. Further *in vitro* antimicrobial activity demonstrated that the cross-linked nonwovens containing TH showed strong activity against bacterial strains associated with periodontal disease. Additionally, the nonwovens did not demonstrate cytotoxic toward fibroblast (HDFn) cells, hence showing their potential for applications as a novel drug delivery platform for periodontitis treatment.

1. Introduction

Periodontitis is an inflammatory disease caused by dental plaque biofilm in the oral cavity that can lead to the progressive destruction of periodontal tissue, including the gingiva, periodontal ligament (PDL), cementum, and alveolar bone [1–3]. Different approaches for treating the periodontal tissues damaged by periodontitis have been pursued including the so-called guided tissue

Abbreviations: $\overline{DD}$, average degree of deacetylation; $\overline{M\nu}$, viscosity average molecular weight; ΔG, interfacial free energy; ANOVA, analysis of variance; ATR-FTIR, attenuated total reflectance Fourier transform infrared spectroscopy; C1, high molecular weight and low deacetylated chitosan; C2, high molecular weight and highly deacetylated chitosan; CA, contact angle; CH, low molecular weight and highly deacetylated chitosan; CH/PVA, non-cross-linked nonwovens without tetracycline and prepared from low molecular weight and highly deacetylated chitosan; CH/PVA-TH, non-cross-linked nonwovens containing tetracycline and prepared from low molecular weight and highly deacetylated chitosan; CL, low molecular weight and low deacetylated chitosan; CL/PVA, non-cross-linked nonwovens without tetracycline and prepared from low molecular weight and low deacetylated chitosan; CL/PVA-TH, CL/PVA-TH non-cross-linked nonwovens containing tetracycline and prepared from low molecular weight and low deacetylated chitosan; CLSI, Clinical and Laboratory Standards Institute; Cp, polymeric concentration; DMEM, Dulbecco's Modified Eagle Medium; FBS, fetal bovine serum; G(CH/PVA), genipin-cross-linked nonwovens without tetracycline and prepared from low molecular weight and highly deacetylated chitosan; G(CH/PVA-TH), genipin-cross-linked nonwovens containing tetracycline and prepared from low molecular weight and highly deacetylated chitosan; G(CL/PVA), genipin-cross-linked nonwovens without tetracycline and prepared from low molecular weight and low deacetylated chitosan; G(CL/PVA-TH), genipin-cross-linked nonwovens containing tetracycline and prepared from low molecular weight and low deacetylated chitosan; GlcN, 2-amino-2-deoxy-D-glucopyranose; GlcNAc, 2-acetamido-2-deoxy-D-glucopyranose; GTR, guided tissue regeneration; HDFn, neonatal human dermal fibroblast cell line; PBS, phosphate-buffered saline solution; PCL, polycaprolactone; PDL, periodontal ligament; PVA, poly (vinyl alcohol); SEM, scanning electron microscopy; TEM, transmission electron microscopy; TH, tetracycline hydrochloride; USAD, ultrasound-assisted deacetylation process; γ^-, electron-donor component; γ^+, electron-acceptor; γ^{AB}, acid-base; γ^{LW}, dispersive component; γ^{TOTAL}, total surface energy.

* Corresponding authors at: Nanotechnology National Laboratory for Agriculture (LNNA), Embrapa Instrumentação, 13560-970 São Carlos, SP, Brazil (D.S. Corrêa).
E-mail addresses: martinsdanilo.9@gmail.com (D.M. dos Santos), daniel.correa@embrapa.br (D.S. Correa).

https://doi.org/10.1016/j.ijbiomac.2019.09.124
0141-8130/

regeneration approach (GTR). The GTR treatment involves the application of a barrier membrane between the gingival epithelium and connective tissues, which prevents migration of the epithelium and gingival connective tissue cells into the defect sites and provides a secluded space for the formation of PDL, cementum and bone [4–6].

According to their degradation profile, GTR membranes are classified into non-resorbable and resorbable, where the latter are more advantageous once they can suppress a second surgical procedure for membrane removal. Collagen-based GTR membranes have demonstrated favorable results due to their excellent biocompatibility, although its use presents some disadvantages such as lack of control on the resorption rate and risk of disease transmission [2,7,8].

Antimicrobial agents are frequently administrated to prevent/treat bacterial infections in periodontal defects. Controlled local delivery of antimicrobials into the defect sites presents many advantages compared to oral administration, including site-specific delivery, decrease of dose requirement and of side effects in the body [9,10]. GTR membranes loaded with antibiotics for local drug release have been reported [11], but many challenges regarding to the correct design of drug release systems still exist.

Biocompatible and biodegradable micro/nanofibers produced by electrospinning, which display high surface area-to-volume ratio, porous structure, mechanical performance, and resemblance to the extracellular matrix, have appeared as potential candidates for GTR using synthetic and natural polymers as well as polymer blends [3,12–16]. In coaxial electrospinning two different solutions are spun simultaneously through two concentrically aligned capillaries to generate core-sheath structured nanofibers or other types of structures, such as hollow nanofibers [17]. Coaxial electrospinning enables the preparation of nanofibers from different type of materials and even from unspinnable liquids, as they can be supplied as the inner or outer fluid to produce nanofibers under the guidance, respectively, of the spinnable outer or inner fluid. This strategy allows the production of core–sheath nanofibers as well as monolithic nanofibers that cannot be produced by a single-fluid process [17–21]. In this regard, coaxial electrospinning has been widely applied to prepare drug delivery systems in which the release of incorporated drug can be modulated by varying the structure and composition of the nanofibers [17–24].

Among different biocompatible and biodegradable polymers that can be used to produce coaxial nanofibers, chitosan is of outmost importance once it is atoxic, and exhibits antimicrobial and hemostatic activities [25,26]. These properties make chitosan one of the most widely studied natural biopolymers for a great variety of biomedical applications including drug delivery systems [27], wound dressings [28,29] and tissue engineering [30]. Chitosan, a β(1 → 4)-linked copolymer of 2-amino-2-deoxy-D-glucopyranose (GlcN) and 2-acetamido-2-deoxy-D-glucopyranose (GlcNAc), is generally prepared by carrying out the *N*-deacetylation of chitin, a polysaccharide abundantly present in the exoskeletons of crustaceans, mollusks and insects [31,32]. The physicochemical properties, the *in vivo* degradation, biological activity and processability of chitosan, are mainly affected by its molecular weight and average degree of deacetylation ($\overline{DD}$), which expresses the number of GlcN units along the chains [33]. Therefore, the properties of chitosan-based biomaterials are strongly dependent on the structural characteristics of this biopolymer.

Despite the potential of chitosan for designing electrospun-based biomaterials, its electrospinnability is largely limited mainly due to repulsive forces between protonated —NH_2 groups pertaining to GlcN units (once the aqueous dilute acid used to dissolve the polymer results in the protonation of such groups). To overcome such a severe limitation, the blend of chitosan with nonionic polymers, such as poly(ethylene oxide) or polycaprolactone (PCL), has been proposed to render the chitosan solution more electrospinnable [34,35]. Additionally, chitosan-based structures generally possess weak mechanical properties and low stability in aqueous medium, which limits its biomedical applications. Chemical and/or physical crosslinking of chitosan is one of the approaches employed to improve the stability of these structures [36,37]. Genipin, a natural crosslinking compound isolated from fruits of *Gardenia jasminoides Ellis* (gardenia) or unripe fruits of *Genipa americana* L. (genipap), has been used to produce self-sustainable, biocompatible, noncytotoxic chitosan-based materials [38–40].

In this context, this study focuses on the development of a drug delivery system based on coaxial electrospun nanofibers intended to be applied as GTR membrane for periodontal regeneration. Tetracycline hydrochloride (TH), a broad-spectrum antibiotic that presents activity against both Gram-positive and Gram-negative bacteria, was chosen as model drug. Two samples of chitosan possessing different average degree of deacetylation ($\overline{DD}$) and similar viscosity average molecular weight ($\overline{Mv}$) were synthesized and coaxially electrospun as shell component (outer layer) while poly (vinyl alcohol) (PVA) loaded with TH was used as the core material (inner layer). PVA was chosen because it is a biocompatible, biodegradable and easily electrospinnable polymer [41,42]. The effects of average degree of deacetylation and post-electrospinning genipin crosslinking on the fibers' structural and physical properties were investigated. The nonwovens were characterized with respect to morphology, surface and mechanical properties, water absorption capacity and biological properties, including cytocompatibility, biodegradability and antibacterial properties, as well as release profile of TH. To the best of our knowledge, there has been no report on the coaxial electrospinning of chitosan possessing different structural characteristics and the evaluation of post-electrospinning genipin crosslinking on the physicochemical, biological and drug release profile.

2. Materials and methods

2.1. Materials

Poly (vinyl alcohol) (PVA), with $\overline{Mw}$ = 31.000–50.000 g mol^{-1}, tetracycline hydrochloride (TH), and lysozyme human (100.000 units/mg) were acquired from Sigma-Aldrich (Saint Louis, MO; USA), while genipin was purchased from Challenge Bioproducts Co. Ltd. (Taiwan, China). Acetic acid (99.8%) was acquired from Synth (Diadema/SP; Brazil). The reactants and solvents employed in this study were used as received.

2.2. Chitosan preparation

Initially, β-Chitin was extracted from squid pens (*Doryteuthis* spp.) by treating the biomass with 1 M aqueous NaOH at room temperature for 18 h as proposed by Chaussard and Domard [43], which was then submitted to cryo-grinding and sieving. Chitosan was prepared by applying the ultrasound-assisted deacetylation (USAD) process to β-chitin particles (0.125 mm < d < 0.250 mm) as described by Fiamingo and Campana-Filho [44]. Briefly, 5 g of β-chitin was suspended in 50 mL of aqueous NaOH (40% w/w) and the suspension was poured into a cylindrical double-walled glass reactor (θint = 3.5 cm) coupled to a circulating thermostat. Following, the suspension was submitted to ultrasound irradiation for 50 min at 60 ± 0.5 °C using the UP400S Hielscher Sonifier ultrasonic device (ν = 24 kHz) coupled to a 22 mm stepped probe, with pulsed irradiation (0.5) and ultrasound power set to 200 W. After

Please cite this article as: D. M. dos Santos, P. A. M. Chagas, I. S. Leite et al., Core-sheath nanostructured chitosan-based nonwovens as a potential drug delivery system for periodontitis treatment, International Journal of Biological Macromolecules, https://doi.org/10.1016/j.ijbiomac.2019.09.124

the ultrasound treatment, the suspension was cooled and neutralized with concentrated hydrochloric acid, filtered and the resulting chitosan was thoroughly washed with water and freeze-dried. This procedure resulted in low deacetylated chitosan (C1), which was submitted to a further USAD processing to result in highly deacetylated chitosan (C2). It is important to highlight that as the multistep USAD process is carried out at relatively low temperature (compared to conventional chemothermal deacetylation of chitin), the USAD chitosans present high molecular weight, well-defined average degree of acetylation and predominant block-wise distribution of GlcN and GlcNAc units.

Owing to the high molecular weight of the USAD chitosans, their solutions presented very high viscosity, precluding its use in the electrospinning experiments. Thus, both USAD chitosans C1 and C2 were submitted to depolymerization via ultrasound treatment as reported in the literature [33], and the so-treated samples presenting lower molecular weight were named as chitosans CL and CH, respectively. The chitosans were characterized and then used in electrospinning experiments. Thus, the average degree of deacetylation ($\overline{DD}$) of C1 and CL was 82%, while for C2 and CH chitosans was 93%, as determined by ^{1}H NMR analysis [45]. The viscosity average molecular weight ($\overline{Mv}$) of the chitosans C1, C2, CL and CH was determined from the corresponding intrinsic viscosity measurements in 0.3 mol L^{-1} acetic acid/0.2 mol L^{-1} sodium acetate buffer (pH 4.5) at 25.00 ± 0.01 °C using the Mark–Houwink–Sakurada equation and taking into account their average degree of acetylation [46]. These experiments revealed that C1 and C2 chitosans presented $\overline{Mv}$ = 325.000 ± 22.000 g mol^{-1} and $\overline{Mv}$ = 290.000 ± 18.000 g mol^{-1}, respectively, while the depolymerized USAD chitosans CL and CH presented $\overline{Mv}$ = 111.000 ± 6.000 g mol^{-1} and $\overline{Mv}$ = 104.000 ± 5.000 g mol^{-1}, respectively.

2.3. Electrospinning process

Chitosan was dissolved in 50 wt% aqueous acetic acid upon stirring for 18 h at room temperature to result in a transparent solution displaying Cp = 40 mg mL^{-1}, which was used to compose the nanofiber shell upon coaxial electrospinning. A PVA solution (Cp = 120 mg mL^{-1}) was prepared in 50 wt% aqueous acetic acid upon stirring for 2 h at 90 °C, which was used after cooling to room temperature to compose the nanofiber core. PVA/ tetracycline hydrochloride (TH) solution was prepared by dissolving TH at a concentration of 10 mg mL^{-1} in the previously prepared PVA solution under constant stirring for 20 min. Prior to electrospinning, the solution conductivities were determined using a conductivity meter (Gehaka, model CG 1800) at 25.0 ± 0.2 °C while the dynamic viscosity (μ, cP) was calculated from the solution flow time (at 25.0 ± 0.2 °C) using a falling-ball viscometer (GILMONT instruments)according to Eq. (1).

$$\mu = K(\rho_{ball} - \rho_{solution})t \quad (1)$$

where ρ_{ball} = density of tantalum ball (16.6 g cm^{-3}); $\rho_{solution}$ = density of spinning solution (g cm^{-3}); t = time of descent of ball (min.); K = viscometer constant (37).

The electrospinning process was carried out in a homemade apparatus composed of a high voltage power supply (Glassman High Voltage, Inc., USA), two syringe pumps (New Era Pump Systems, Inc., USA) to control the flow rates of core and sheath fluids, and a metallic drum collector to collect the nanofibers. For coaxial electrospinning, the solutions of chitosan and PVA/TH (or PVA solution) were transferred into 3 mL syringes, and pumped separately through the concentrically aligned outer and inner needle, respectively. Diameters of the outer and the inner needle were 1.02 mm and 0.65 mm, respectively. The flow rate of the shell solution was set at 10 μL min^{-1}, while that of the inner fluid was 5 μL min^{-1}. A working distance of 5 cm was kept between the needle and the collector and a voltage of 25 kV was applied. Fibers were directly electrospun onto the stainless-steel drum collector (L = 15.0 cm, W = 7.3 cm, rotation at ≈180 rpm) covered with an aluminum foil. All experiments were carried out during 2 h 40 min. at 25 ± 3 °C and a relative humidity of 25–40%. After electrospinning, the resulting nonwovens were carefully removed from the aluminum foil, dried at 30 °C for 12 h and stored in a desiccator before further use. The resulting nonwovens containing tetracycline were named as CL/PVA-TH and CH/PVA-TH, while those without antibiotic were named as CL/PVA and CH/PVA, respectively.

2.4. Crosslinking treatment using genipin

Core-sheath electrospun nanofibrous nonwovens were crosslinked upon immersion in genipin ethanolic solution (5 mg mL^{-1}) at room temperature for 15 min. Next, an excess of absolute ethanol was used to wash away the samples after the crosslinking reaction. Then, the cross-linked nonwovens were dried at 30 °C for 12 h and stored in a desiccator. The genipin cross-linked nonwovens were named as G(CL/PVA), G(CH/PVA), G(CL/PVA-TH) and G(CH/PVA-TH).

2.5. Characterization

2.5.1. Morphology of nanofibers

The fibers' morphology was investigated with a scanning electron microscope (SEM, JEOL 6510) using an acceleration voltage of 10 kV after sputter coating the samples with gold. The fibers' average diameter was determined from the SEM images using ImageJ 1.45 software (National Institutes of Health, Bethesda, MD, USA), measuring at least 150 random fibers from 6 micrographs of each nonwoven. The Core-sheath structure of the fibers was characterized by transmission electron microscopy (TEM, JEOL JEM2100 LaB6) with an acceleration voltage of 200 kV. To prepare the samples for TEM analysis, the fibers were deposited directly onto 300-mesh carbon-coated Cu grids.

2.5.2. Attenuated total reflectance Fourier transform infrared spectroscopy

ATR-FTIR spectra of electrospun nonwovens were recorded on a Bruker vertex 70 spectrometer using a universal attenuated total reflection (ATR) accessory. Spectra were recorded between 4000 and 600 cm^{-1} by the accumulation of 32 scans and a resolution of 4 cm^{-1}.

2.5.3. Contact angle, surface and interfacial free energy

Contact angle (CA) measurements were carried out using a goniometer (CAM 2008, KSV) equipped with CAM 2008 software. Nonwovens samples (15 mm × 10 mm) were attached to glass slides and apparent contact angles were determined from the sessile profile droplets (approx. 3 μL) of three liquids of different polarities (deionized water, diiodomethane and ethylene glycol) 1 s after deposition. Each sample was evaluated at five different points at room temperature. Contact angle data and the surface tension components of the probe liquids (γ_L, γ_L^{LW}, γ_L^-, γ_L^+) [47] were used to calculate the nonwovens surface free energy and surface energy components using the van Oss, Chaudhery and Good model [48] as described by [49]. Briefly, the total surface energy (γ^{TOTAL}) was calculated by the sum of the apolar (γ^{LW}) and polar (γ^{AB}) components ($\gamma^{TOTAL} = \gamma^{LW} + \gamma^{AB}$), the latter being calculated from electron acceptor component (γ^+) and electron donor component (γ^-). The hydrophobicity (hydrophilicity) of surface nonwovens was quantitatively assessed from the interfacial free energy (ΔG),

Please cite this article as: D. M. dos Santos, P. A. M. Chagas, I. S. Leite et al., Core-sheath nanostructured chitosan-based nonwovens as a potential drug delivery system for periodontitis treatment, International Journal of Biological Macromolecules, https://doi.org/10.1016/j.ijbiomac.2019.09.124

which was determined from surface energy components of nonwovens (γ_S^{LW}, γ_S^-, γ_S^+) and surface tension parameters of deionized water (γ_W^{LW}, γ_W^-, γ_W^+) [50].

2.5.4. Swelling capacity

The swelling behavior of the nonwovens was assessed using a gravimetric method proposed by Dos Santos et al. (2018) with modifications. Nonwovens were cut into strips (2 cm × 2 cm), weighted and then immersed in 25 mL of phosphate-buffered saline (PBS), pH 7.4 at 37 °C in an incubator. At predetermined time up to 30 min., the samples were taken out of the fluid, blot dried and weighed. The swelling ratio was calculated according to Eq. (2). Five repeats of each nonwoven composition were evaluated.

$$\text{Swelling Ratio } (\%) = ((W_{wet} - W_{dry})/W_{dry}) \times 100 \quad (2)$$

where W_{dry} and W_{wet} correspond to the weight of dried and swollen mats, respectively.

2.5.5. In vitro enzymatic degradation

The *in vitro* biodegradability of nonwovens was studied by incubating them at 37 °C for 14 days in phosphate-buffered saline (PBS, pH = 7.4) containing lysozyme (276 mg L^{-1}). Nonwovens strips (2 cm × 2 cm) were weighed and placed into individual vials (20 mL) containing 5 mL of buffer solution. At predetermined times (6 h, 12 h, 1, 2, 4, 7 and 14 days), samples were removed from the buffer, washed with deionized water, freeze-dried at −55 °C for 48 h, and weighed. The mass percent remaining of the nonwoven was calculated according to Eq. (3). Control tests, which correspond to incubation in the absence of lysozyme, were also carried out. All experiments were carried out in triplicate.

$$\text{Mass remaining } (\%) = (W_t/W_0) \times 100 \quad (3)$$

where W_0 is the initial weight of the nonwoven and W_t is its weight after degradation.

2.5.6. Tensile properties

Tensile tests of rectangular specimens of nonwovens (20 mm × 6.4 mm) were carried out using a Q800 from TA Instruments in tension mode using a thin film clamp at 25 °C. The distance between grips was kept at 5 mm, and the tests were carried out with ramp strength of 1 N/min up to 18 N. At least five samples were evaluated for each specimen and the tensile strength (MPa), elastic modulus (MPa) and elongation-at-break (%) were determined from stress-strain curves.

2.5.7. In vitro drug release study

In vitro release of tetracycline hydrochloride (TH) was evaluated by immersing 10 mg of nonwovens in 7 mL phosphate-buffered saline (PBS, pH = 7.4) containing lysozyme (276 mg L^{-1}) at 37 °C under shaking at 60 rpm in an incubator. At predetermined time intervals, an aliquot of the medium (0.7 mL) was withdrawn and replaced by fresh solution. The amount of TH released in the incubation medium was quantified using UV spectrophotometry (Shimadzu, UV-1800) at 360 nm based on a previously prepared calibration curve. Control tests, which correspond to incubation in the absence of lysozyme, were also carried out. Each experiment was performed in triplicate and the results were expressed in terms of cumulative release as a function of release time.

2.5.8. Cell viability study

Neonatal human dermal fibroblast cell line (HDFn, Gibco®, cat. n°C0045C) was acquired from Thermo Fischer Scientific (Waltham, MA, USA). The cells were tested between passages 15 and 20 and were grown continuously in humidified incubator (MCO-17AC, Sanyo Electric Co. Ltd., Osaka, Japan) at 37 °C and 5% CO_2 atmosphere with Dulbecco's Modified Eagle Medium (DMEM) supplemented with 10% (v/v) fetal bovine serum (FBS) and 0.5% (v/v) penicillin-streptomycin, all purchased from Cultilab (Campinas, SP, Brazil). Cell viability experiments were carried out according to the protocol adapted from ISO 10993-5 [51] and described by Neamnark et al. [52]. In brief, cross-linked nonwovens strips (20 mm × 20 mm) were sterilized with ethanol and extracts were prepared through 24 h of incubation with fresh phenol-red free DMEM supplemented with 10% FBS at 37 °C and 5% CO_2 atmosphere (extraction ratio: 4 mg mL^{-1}). Simultaneously, 96 well-plates were seeded with 5×10^4 cells mL^{-1} in DMEM supplemented with 10% FBS and incubated in humidified incubator at 37 °C and 5% of CO_2 for 24 h. Cell medium was then replaced by 100 μL of pure (4 mg/mL) or serial diluted nonwovens extracts (4, 2, 1, 0.5 and 0.1 mg mL^{-1}) or phenol-red free DMEM with 10% FBS (control group) and the plates were incubated for 24 h in humidified incubator. Cell viability was assessed indirectly by the MTT assay (stock solution: 5 mg mL^{-1}). Absorbance values were measured with the microplate spectrophotometer MultiskanTM GO (Thermo Fischer Scientific) at 570 nm, and viability values were calculated considering the absorbance values of the control group (i.e., cells cultured in medium without nonwovens extracts) as 100% of viability. Experiments were conducted in triplicates of each group and repeated in three different occasions (total n = 9).

2.5.9. Antibacterial activity experiments

2.5.9.1. Activity test against periodontal pathogens. The antibacterial activities of the nanofibrous nonwovens against a series of bacterial strains associated with periodontal disease obtained from human periodontal subgingival pocket of patients with chronic periodontitis were evaluated according to the protocol established by Clinical and Laboratory Standards Institute (CLSI) [53] Initially, clinical samples were collected from human periodontal subgingival pocket of three patients presenting at least 10 periodontal sites with bleeding and probing depth ≥5 mm. Patients spontaneously adhered to this study and to select them, the following criteria were adopted: absence of positive history of antibiotic use or any type of periodontal treatment at least 3 months prior to this study as well as immunosuppressive diseases or systemic changes evident on clinical examination or detected by anamnesis. The Ethics and Research Committee of the Sao Paulo State University (UNESP) approved the collection of plaque samples and all patients signed free informed consent in accordance with Resolution No. 196/96 of the Directives and Norms of the National Health Council.

Subgingival plaques were collected from the premolars and molars using Gracey's curettes and suspended in sterile saline solution. After this treatment, the resulting suspension was centrifuged and a portion of plaque pellet was resuspended in 150 μL of Tris-EDTA buffer solution (10 mM Tris, 1 mM EDTA) (pH 7.6) and 100 μL of 0.5 mol L^{-1} NaOH, and then submitted to checkerboard DNA-DNA hybridization analysis according to the methodology proposed by Socransky et al. [54] in order to identify the bacterial strains present in periodontal plaques. Nonwovens disks (ϕ = 10 mm, n = 3/group) were used in order to assess the growth inhibition toward bacterial strains associated to periodontitis. For these experiments, subgingival plaques pellets previously prepared were resuspended in brain-heart infusion broth and suspension concentration was adjusted to $\approx 1 \times 10^8$ cell mL^{-1}. Then, the surface of a supplemented sheep blood agar plate was uniformly seeded with a sterile cotton swab containing the microorganisms and samples of each nonwovens were placed on the agar plate, which was incubated under anaerobic condition (80% N_2 − 10% CO_2 − 10% H_2) at 37 °C for 4 days. After incubation, each plate was examined to evaluate the growth inhibition of microorganisms in regions around the nonwovens, according to the pres-

Please cite this article as: D. M. dos Santos, P. A. M. Chagas, I. S. Leite et al., Core-sheath nanostructured chitosan-based nonwovens as a potential drug delivery system for periodontitis treatment, International Journal of Biological Macromolecules, https://doi.org/10.1016/j.ijbiomac.2019.09.124

ence or absence of inhibition zones, which was considered the area with absence of growth detectable by the naked eye.

2.6. Statistical analysis

All data were expressed as the mean ± standard deviation. In order to check for any statistically significant differences, an one-way analysis of variance (ANOVA) was performed followed by Tukey's post hoc test at the 95% confidence level using an open-source statistical programming language R v. 3.1.1.

3. Results and discussion

3.1. Conductivity and viscosity of spinning solutions

Coaxial electrospinning technique was employed to prepare chitosan-based core-sheath nanofibers aiming to develop a novel drug delivery platform for periodontitis treatment. Two different chitosans possessing well-defined characteristics in terms of average degree of deacetylation ($\overline{DD}$) and viscosity average molecular weight ($\overline{Mv}$) were used to prepare the solutions employed for electrospinning the shell of the nanofibers while solutions of PVA or PVA/TH were coaxially electrospun to produce the core layer. The optimized electrospinning parameters were defined by subsidiary experiments (results not shown), where parameter effects such as electric field strength, polymer concentration and flow rate were investigated. Based on these experiments, the applied voltage and spinneret-to-collector distance were fixed at 25 kV and 5 cm, respectively, while the flow rate of the shell and core solutions were set at 10 μL min^{-1} and 5 μL min^{-1}, respectively, which allowed the production of nonwovens composed by nanofibers displaying the aimed core-sheath structure.

The physicochemical properties of polymer solution, mainly its conductivity, and viscosity, play a crucial role in the electrospinning process. In this sense, the conductivity and viscosity of spinning solutions were measured as shown in Fig. 1. As expected, the conductivity of PVA solution increased by addition of TH due to its ionic character, while solution viscosity was not affected by antibiotic presence. Results also reveal that shell solution conductivity increases with increasing the average degree of acetylation of chitosan, which is attributed to the higher content of protonated amino groups of 2-amino-2-deoxy-D-glupyranose units pertaining to the parent chitosan [49,55]. The solution viscosity of shell solutions was not affected by their composition and this behavior can be explained by the similar values of viscosity average molecular weight ($\overline{Mv}$) of parent chitosans.

3.2. Morphology and core-sheath structure of nanofibers

The surface morphology of nonwovens was analyzed by scanning electron microscopy (SEM), which representative micrographs are displayed in Fig. 2. The morphological analysis revealed the non-cross-linked nonwovens as densely packed network-like structures composed by smooth bead-free nanofibers. The corresponding fiber diameter histograms show that the fibers' diameter is predominantly in the range 100−250 nm, except in the case of nonwoven CH/PVA sample, whose fiber diameter range is wider (150–350 nm). The morphology and diameter of electrospun fibers are strongly affected by the conductivity and viscosity of spinning solutions and an adequate combination of both parameters is fundamental to yield defect-free, beadless, and geometrically uniform fibers [56]. In this sense, the changes in fiber morphology and size distribution observed for CH/PVA nonwoven can be attributed to the low conductivity of PVA solution, which leads to the ejection of thicker jets, and to the high conductivity and viscosity of spinning solution prepared from highly deacetylated chitosan (CH), which increases the instability of the ejected jets, thus increasing the broadness of fiber diameter distribution.

After crosslinking with genipin, the homogeneous fibrous structure of nonwovens was retained, but a slight change in fiber morphology and diameter distribution was observed in all cases as a consequence of the crosslinking (Fig. 2a). Such behavior was more pronounced in the case of nonwoven G(CH/PVA-TH), whose average fiber diameter was higher (234 ± 54 nm) as compared to that of CH/PVA-TH nonwoven (174 ± 33 nm), and a broader fiber diameter distribution was observed. The slight change in fiber diameter

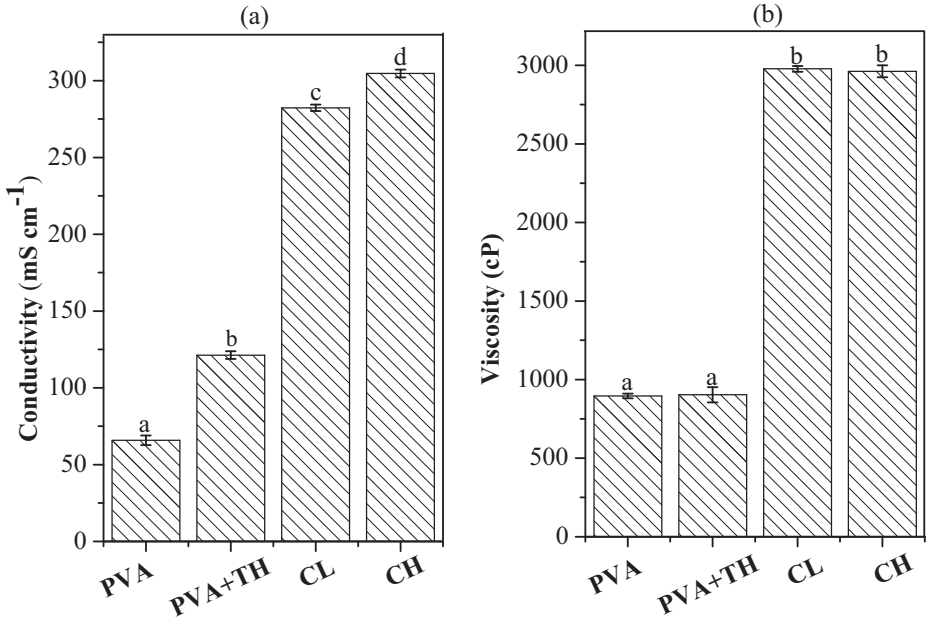

Fig. 1. Conductivity (a) and dynamic viscosity (b) of the spinning solutions. Means followed by the same letter in the columns do not differ by a Tukey's test at the 95% confidence level.

Please cite this article as: D. M. dos Santos, P. A. M. Chagas, I. S. Leite et al., Core-sheath nanostructured chitosan-based nonwovens as a potential drug delivery system for periodontitis treatment, International Journal of Biological Macromolecules, https://doi.org/10.1016/j.ijbiomac.2019.09.124

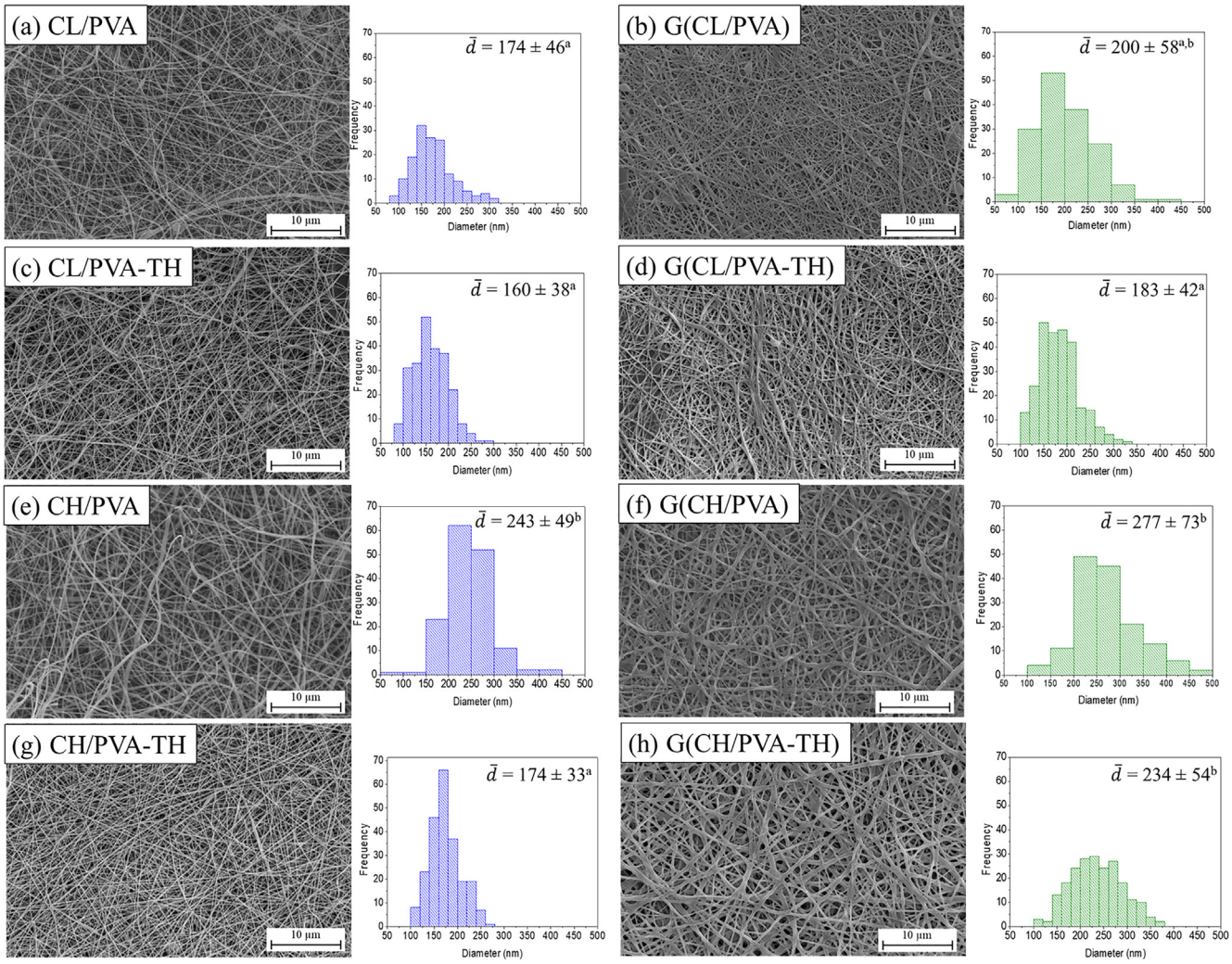

Fig. 2. SEM micrographs of non-cross-linked nonwovens (CL/PVA (a), CL/PVA-TH (c), CH/PVA (e), CH/PVA-TH (g)) and cross-linked nonwovens (G(CL/PVA) (b), G(CL/PVA-TH) (d), G(CH/PVA) (f), G(CH/PVA-TH) (h)), as well as the corresponding histograms showing fiber diameter distributions.

and morphology may have resulted from ethanol uptake in the nonwoven due to their porous structure, causing swelling of fibers. The morphological differences observed between G(CH/PVA-TH) and G(CL/PVA-TH) can be explained by the structural characteristics of parent chitosan. Indeed, since CL is less deacetylated ($\overline{DD}$ = 82%) than CH ($\overline{DD}$ = 93%), the crosslinking process is favored for the latter due to the higher content of amino groups of 2-amino-2-deoxy-D-glupyranose units. In such case, there is a reduction of the interpenetration between genipin cross-linked chitosan and PVA-TH layers, thus favoring the expansion of PVA-TH network due to its higher affinity to ethanol, which results in an increase of G(CH/PVA-TH) fiber diameter.

Transmission electron microscopy (TEM) was used to confirm the Core-sheath structure of nanofibers. TEM micrographs (Fig. 3) of cross-linked and non-cross-linked fibers exhibit a clear bilayer structure with the inner layer showing a dark gray color and the outer layer showing a light gray color, thus indicating that the coaxial electrospinning was successful and that the integrity of core-sheath structure of fibers was kept after crosslinking with genipin.

3.3. ATR-FTIR analysis

The ATR-FTIR spectra of less deacetylated chitosan (CL), PVA and TH in powder form as well as those of the nonwovens CL/PVA-TH and G(CL/PVA-TH) are compared in Fig. 4a to give insight on the characteristics functional groups of nonwovens. The spectrum of chitosan exhibits an absorption band centered at 1658 cm^{-1} related to the C=O stretching of amide I and a band at 1590 cm^{-1} that corresponds to N—H bending of primary amine [57,58]. The spectrum of PVA shows a typical band at 1423 cm^{-1} related to the bending of the C—H bond of methylene groups [59]. The spectrum of TH exhibits characteristic absorption bands at 1676, 1613, 1577, 1530 and 1448 cm^{-1} due to the C=O vibration of Amide I, C=O vibration of aromatic ring, C=O vibration of C-ring, NH_2 deformation of Amide II and C=C vibration of aromatic ring, respectively [60]. Accordingly, the spectra of CL/PVA-TH and G(CL/PVA-TH) nonwovens show absorption bands at 1658 cm^{-1} and 1590 cm^{-1}, characteristic of chitosan, and a band at 1423 cm^{-1} related to the presence of PVA. However, the low content of TH impairs the clear identification of its characteristics bands on G(CL/PVA-TH) nonwoven spectrum. In addition, the bands corresponding to the primary amine (at 1590 cm^{-1}) and to amide I (at 1658 cm^{-1}) are less and more intense, respectively, in the spectrum of G(CL/PVA-TH) nonwoven (Fig. 4b). Such facts indicate that some primary amine groups of GlcN units of chitosan have been consumed by the reaction with genipin to result in crosslinking and to form secondary amine groups. Indeed, taking into account the conditions used in this study to carry out the crosslinking reaction, its mechanism involves the nucleophilic

Please cite this article as: D. M. dos Santos, P. A. M. Chagas, I. S. Leite et al., Core-sheath nanostructured chitosan-based nonwovens as a potential drug delivery system for periodontitis treatment, International Journal of Biological Macromolecules, https://doi.org/10.1016/j.ijbiomac.2019.09.124

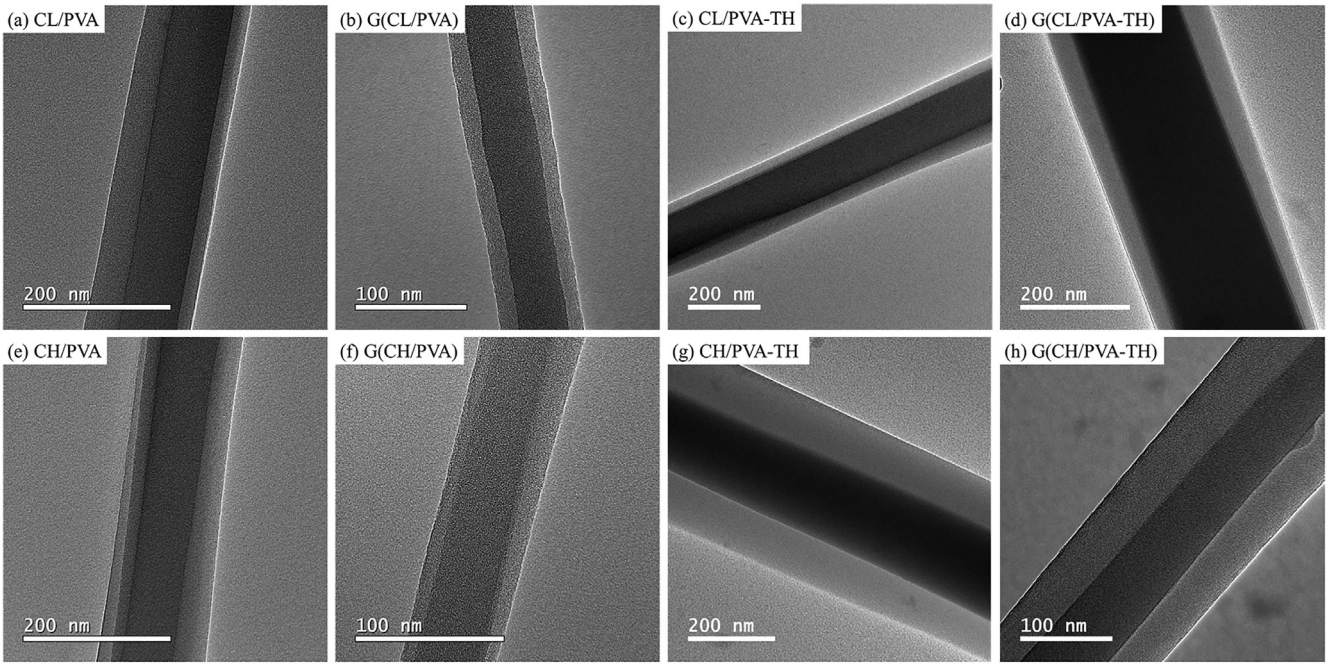

Fig. 3. TEM micrographs of core-sheath non-cross-linked nanofibers (CL/PVA (a), CL/PVA-TH (c), CH/PVA (e), CH/PVA-TH (g)) and cross-linked (G(CL/PVA) (b), G(CL/PVA-TH) (d), G(CH/PVA) (f), G(CH/PVA-TH) (h)) nanofibers.

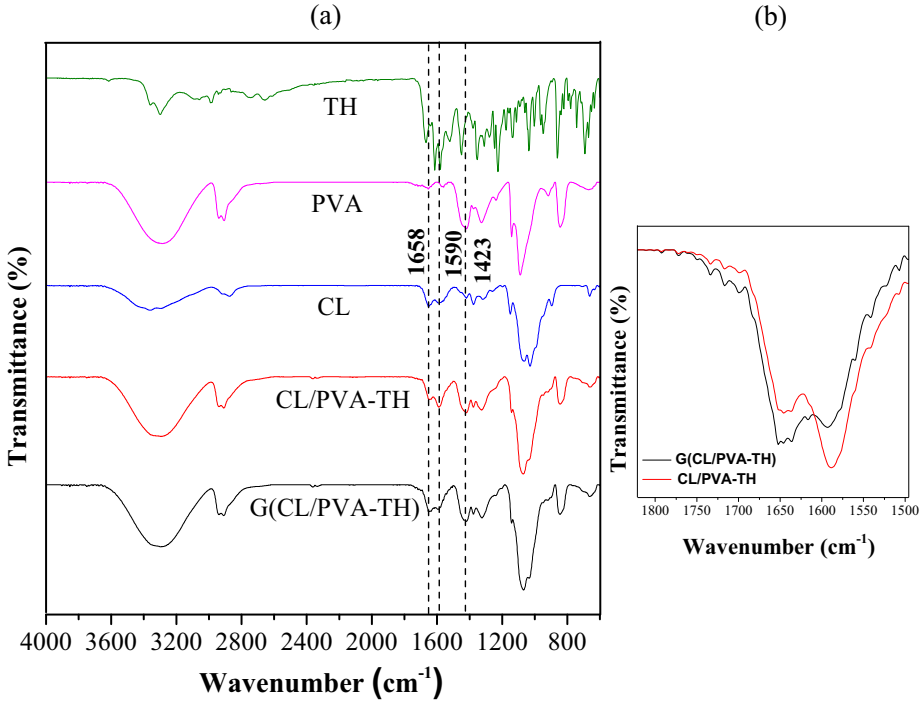

Fig. 4. ATR-FTIR spectra of TH, PVA and chitosan CL in the powder form and of CL/PVA-TH and G(CL/PVA-TH) nonwovens (a); ATR-FTIR spectra magnification in the range 1800–1500 cm^{-1} showing the comparison between cross-linked and non-cross-linked nonwovens (b).

attack of amino groups pertaining to GlcN units of chitosan to the olefinic carbon atom at C-3 of genipin and the subsequent opening of the dihydropyran ring followed by a nucleophilic attack of the secondary amino group to the newly formed aldehyde group, resulting in a cross-linked polymer network [61]. It is important to highlight that comparing the spectra of the other cross-linked and non-cross-linked nonwovens revealed the same trend as that observed in the comparison of nonwovens CL/PVA-TH and G(CL/PVA-TH).

3.4. Surface free energy and hydrophilicity of nonwovens

The nonwoven surface free energy and surface energy components (Table 1) were determined from contact angle (CA) measure-

Please cite this article as: D. M. dos Santos, P. A. M. Chagas, I. S. Leite et al., Core-sheath nanostructured chitosan-based nonwovens as a potential drug delivery system for periodontitis treatment, International Journal of Biological Macromolecules, https://doi.org/10.1016/j.ijbiomac.2019.09.124

Table 1
Surface energy components* and interfacial free energy of interaction (ΔG) of nonwovens (in mJ m^{-2}).

Sample**	γ^{LW}	γ^{+}	γ^{-}	γ^{AB}	γ^{TOTAL}	ΔG
CL/PVA	36.7 ± 0.2[a]	0.17 ± 0.01[a]	72.2 ± 0.9 [a]	7.1 ± 0.3[a]	43.8 ± 0.5[a]	60.1 ± 0.6[a]
G(CL/PVA)	39.7 ± 0.6[b]	0.04 ± 0.01[b]	31.3 ± 0.7[b]	2.5 ± 0.1[b]	42.0 ± 0.9[a]	5.2 ± 0.8[b]
CL/PVA-TH	34.2 ± 0.1[c]	0.14 ± 0.01[c]	70.4 ± 0.9 [a]	6.3 ± 0.2[c]	40.5 ± 0.1[b]	59.7 ± 0.9[a]
G(CL/PVA-TH)	41.0 ± 0.8[d]	0.13 ± 0.03[c]	38.9 ± 0.9[c]	4.5 ± 0.6[d]	44.1 ± 3.2[a]	16.6 ± 0.4[c]
CH/PVA	36.1 ± 0.8[a]	0.05 ± 0.02[b]	68.4 ± 0.3[d]	4.3 ± 0.3[d]	39.2 ± 1.6[b]	59.1 ± 1.0 [a]
G(CH/PVA)	41.0 ± 0.1[d]	0.05 ± 0.01[b]	30.5 ± 0.3[b]	2.3 ± 0.3[b,f]	43.3 ± 0.4[a]	3.4 ± 0.1[d]
CH/PVA-TH	38.4 ± 0.3[e]	0.21 ± 0.01[d]	71.3 ± 4.4[a]	7.9 ± 0.1[e]	46.5 ± 0.1[c]	60.3 ± 0.4[a]
G(CH/PVA-TH)	39.4 ± 0.4[b]	0.04 ± 0.004[b]	31.6 ± 2.5[b]	2.2 ± 0.1[f]	40.9 ± 0.9[a]	3.5 ± 0.9[d]

* Dispersive (γ^{LW}), electron-donor (γ^{-}), electron-acceptor (γ^{+}), acid-base (γ^{AB}); total surface energy (γ^{TOTAL}).
** Means followed by the same letter in the columns do not differ by a Tukey's test at the 95% confidence level.

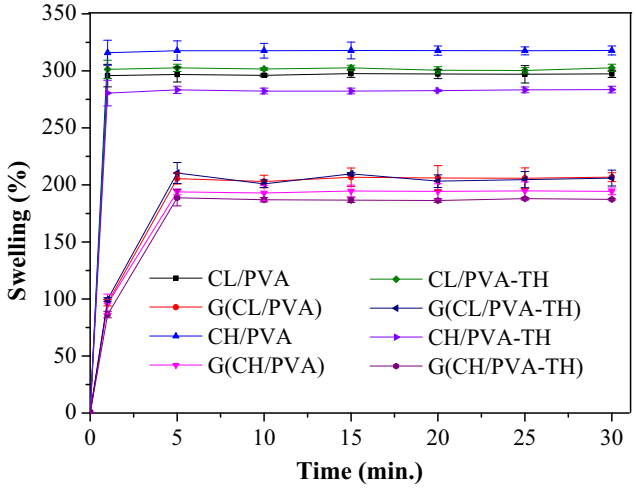

Fig. 5. Swelling behavior of non-cross-linked (CL/PVA, CL/PVA-TH, CH/PVA, CH/PVA-TH) and cross-linked (G(CL/PVA), G(CL/PVA-TH), G(CH/PVA), G(CH/PVA-TH) nonwovens in phosphate-buffered saline (PBS), pH 7.4 at 37 °C.

ments (Table S1, Supplementary data) by probing three liquids of different polarities, namely water, ethylene glycol and diiodomethane, and by using the method proposed by Good, van Oss and Chaudhery [48].

Surface free energy components of nonwovens are related to many interfacial processes such as absorption and wetting of aqueous fluids, thus influencing their applications in biomedical field. As can be seen in Table 1, for all nonwovens the contribution of the dispersive component (γ^{LW}), which accounts the capacity of the surface to take part in London or dispersive interactions, to the total surface energy (γ^{TOTAL}) is higher than the contribution of the polar component (γ^{AB}), which is associated to all the other possibilities of interactions (induction, dipole, and hydrogen bonding). Results also reveal that the polar component contribution to total surface energy decreased upon crosslinking the nonwovens. A similar trend was also observed concerning the electron-donor component (γ^{-}) of the polar component. Additionally, the electron-donor component of the polar surface energy dominated over the electron-acceptor (γ^{+}) one ($\gamma^{-}/\gamma^{+} \gg 1$), thus indicating that the surface of the nonwovens possesses strong electron donating capacity and ability to participate in polar interactions with acid species [47,50].

The interfacial free energy (ΔG) of the nonwovens was calculated in order to evaluate the hydrophilic or hydrophobic nature of theirs surfaces. By thermodynamic convention, when $\Delta G > 0$ the interaction of the material surface with water dominates and the surface of the material is hydrophilic, while $\Delta G < 0$ indicates that the interaction of surface components (cohesive attraction) of the material is favored rather than forming an interface with water. Results expressed in Table 1 demonstrate that $\Delta G > 0$ for all nonwovens and that the increase of average degree of deacetylation for chitosan did not affect ΔG values. However, genipin crosslinking resulted in reduction of interfacial free energy values, which indicates that less hydrophilic groups are exposed at the surface of the cross-linked nonwovens. This behavior corroborates the results from ATR-FTIR spectroscopy, which evidenced the band intensity decrease due to amino groups of GlcN units because of genipin crosslinking. Taking into account the whole set of results, the decrease of hydrofilicity may be considered a desirable attribute for enhancing the stability of these materials in aqueous medium and to control the release of hydrophilic drugs incorporated inside the core layer of nanofibers.

3.5. Swelling behavior

A GTR membrane should have adequate fluid absorption capacity regarding its exposition to blood and body fluids during its application. In this regard, the swelling capacity of nonwovens was investigated by immersing them into PBS at 37 °C, and the results are summarized in Fig. 5. As can be seen, all nonwovens were able to quickly absorb PBS as the swelling equilibrium condition was reached in 1 min. and 5 min. in the cases of non-cross-linked and cross-linked nonwovens, respectively. Results also reveal that the maximum swelling capacity decreased upon crosslinking, which is attributed to the decrease of the hydrophilic character of nonwovens. In addition, CH/PVA and CH/PVA-TH nonwovens exhibited, respectively, the highest and lowest maximum swelling capacity among the non-cross-linked nonwovens, while no significant difference was observed when comparing CL/PVA and CL/PVA-TH nonwovens. After crosslinking, the maximum swelling capacity values were not significantly affected by structural characteristics of chitosan and by the presence of antibiotic. Overall, the decrease of swelling capacity upon crosslinking is advantageous, since high swelling ratios are not favorable because the space occupied in site defect by the GTR membranes is limited and higher fluid absorption may lead to higher infiltration of fibroblast cells, thus hindering an adequate periodontal regeneration [11].

3.6. In vitro biodegradability

Determination of the *in vitro* degradability of the nonwovens allows the prediction of their stability in aqueous medium, which is suitable to avoid their removal by an additional surgical procedure and to provide space for newly formed tissues [7,11]. Aiming to simulate real conditions of application, the *in vitro* biodegradability of nonwovens was evaluated in a phosphate buffer solution (pH 7.4) at 37 °C for 14 days in the absence and presence of lysozyme (276 mg/L) as presented in Fig. 6a and 6b, respectively. The lysozyme concentration used in this study corresponds to that found in gingival crevicular fluid [62–64]. Lysozyme is an impor-

Please cite this article as: D. M. dos Santos, P. A. M. Chagas, I. S. Leite et al., Core-sheath nanostructured chitosan-based nonwovens as a potential drug delivery system for periodontitis treatment, International Journal of Biological Macromolecules, https://doi.org/10.1016/j.ijbiomac.2019.09.124

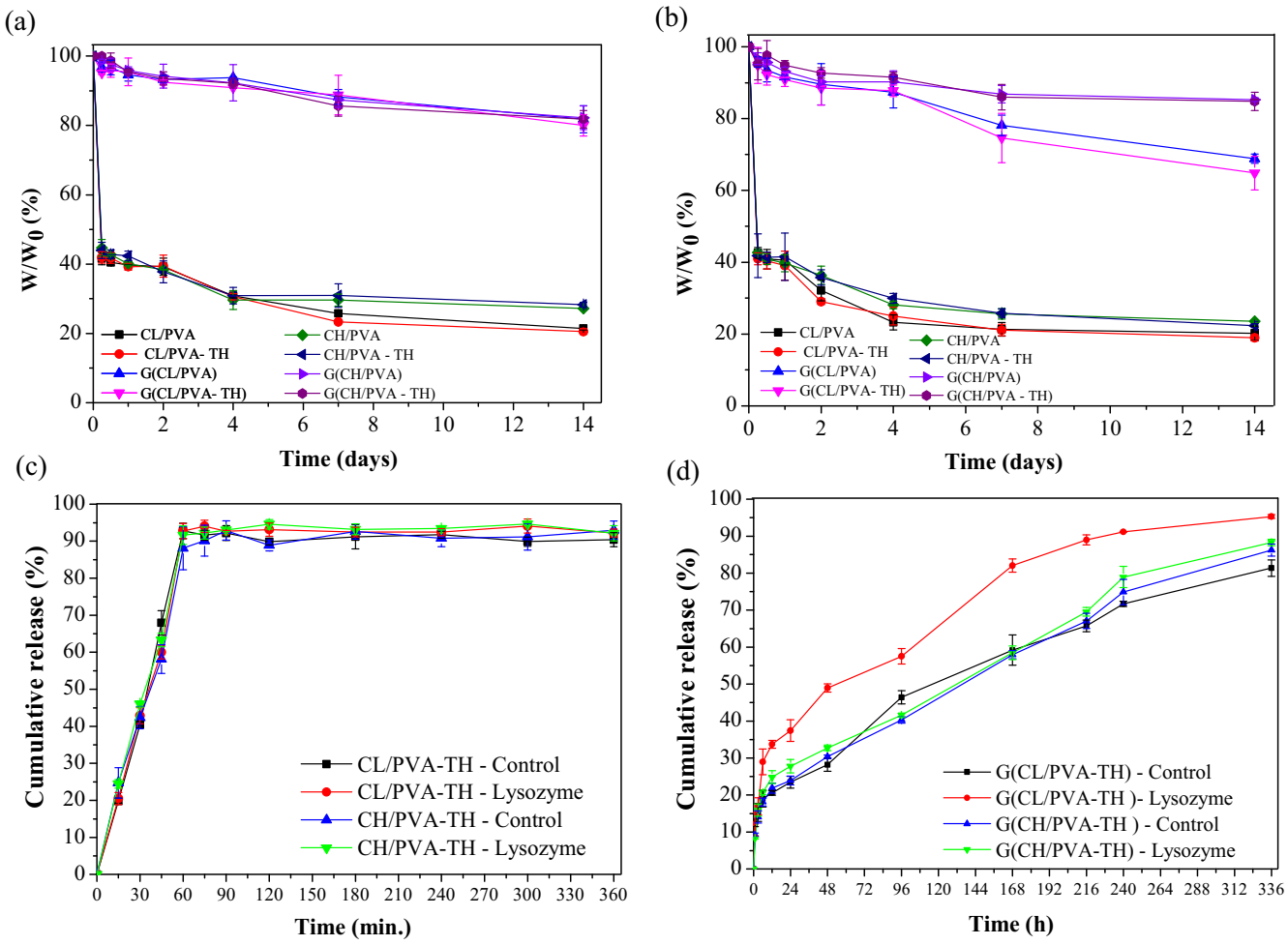

Fig. 6. *In vitro* degradation profiles of non-cross-linked (CL/PVA, CL/PVA-TH, CH/PVA, CH/PVA-TH) and cross-linked (G(CL/PVA), G(CL/PVA-TH), G(CH/PVA), G(CH/PVA-TH) nonwovens in the absence (a) and presence (b) of lysozyme in a phosphate buffer solution (pH 7.4) at 37 °C; Cumulative release profile of tetracycline hydrochloride from non-cross-linked (CL/PVA, CL/PVA-TH, CH/PVA, CH/PVA-TH) (c) and cross-linked (G(CL/PVA), G(CL/PVA-TH), G(CH/PVA), G(CH/PVA-TH) (d) nonwovens in the absence (control) and presence of lysozyme.

tant defense enzyme that acts against some pathogens, mainly Gram-positive bacteria, and it is able to degrade chitosan-based materials by hydrolyzing β (1 → 4) glycosidic bond between GlcN and GlcNAc units [25,64,65]. The *in vitro* degradation profiles of nonwovens are presented in Fig. 6 and reveal that genipin crosslinking expressively improves the stability of materials in aqueous medium.

A substantial higher weight loss was observed in the cases of non-cross-linked nonwovens after 1 day in the presence as well as in the absence of lysozyme (remaining weight <45%) as compared to cross-linked nonwovens, which remaining weight was higher than 92% in both incubation media. In the absence of lysozyme, the degradation profile of cross-linked nonwovens did not differ significantly, regardless of acetylation average degree of chitosan and presence of tetracycline hydrochloride, where the remaining weight lied close to 85% after 14 days of incubation. On the other hand, the structural characteristics of chitosan strongly affect the weight loss profile of cross-linked nonwovens in the presence of lysozyme as demonstrated by the increase of stability of the nonwovens with increasing of the degree of deacetylation. Thus, after 14 days of incubation the remaining weights of nonwovens G(CL/PVA) and G(CL/PVA-TH) were both quite low (≈65%) as compared to those of G(CH/PVA) and G(CH/PVA-TH) nonwovens (≈85%). Such a behavior is explained by the high content of sequences of diads GlcNAc/GlcNAc in the chains of chitosan CL ($\overline{DD}$ = 82%) as compared to CH (DD = 93%), which favors the lysozyme activity [65,66]. Considering that GTR membrane must be stable for at least 4–6 weeks to allow successful regeneration of the periodontal system, it can be concluded that nonwovens G(CH/PVA) and G(CH/PVA-TH) present higher potential to be used in periodontal regeneration [7,11].

3.7. In vitro drug release

As demonstrated in Section 3.6, lysozyme is able to degrade chitosan-based nonwovens, which may affect the release of tetracycline hydrochloride (TH) from nonwovens. In this sense, the drug release experiments were carried out in the presence as well as in the absence of lysozyme. The cumulative percentage of TH released from non-cross-linked (Fig. 6c) and cross-linked nonwovens (Fig. 6d) reveals very different release behaviors. Indeed, regardless of non-cross-linked nonwoven composition and incubation medium, approximately 90% of TH was released within 60 min. Such results indicate that the release of TH from non-crosslinked nonwovens initially involves the swelling of polymer matrix, which facilitates the solvent access to the drug incorporated in the polymeric matrix and the release of drug by diffusion mechanism. In addition, the lack of stability of these materials in aqueous medium, as evidenced by *in vitro* degradability study, also contributed

Please cite this article as: D. M. dos Santos, P. A. M. Chagas, I. S. Leite et al., Core-sheath nanostructured chitosan-based nonwovens as a potential drug delivery system for periodontitis treatment, International Journal of Biological Macromolecules, https://doi.org/10.1016/j.ijbiomac.2019.09.124

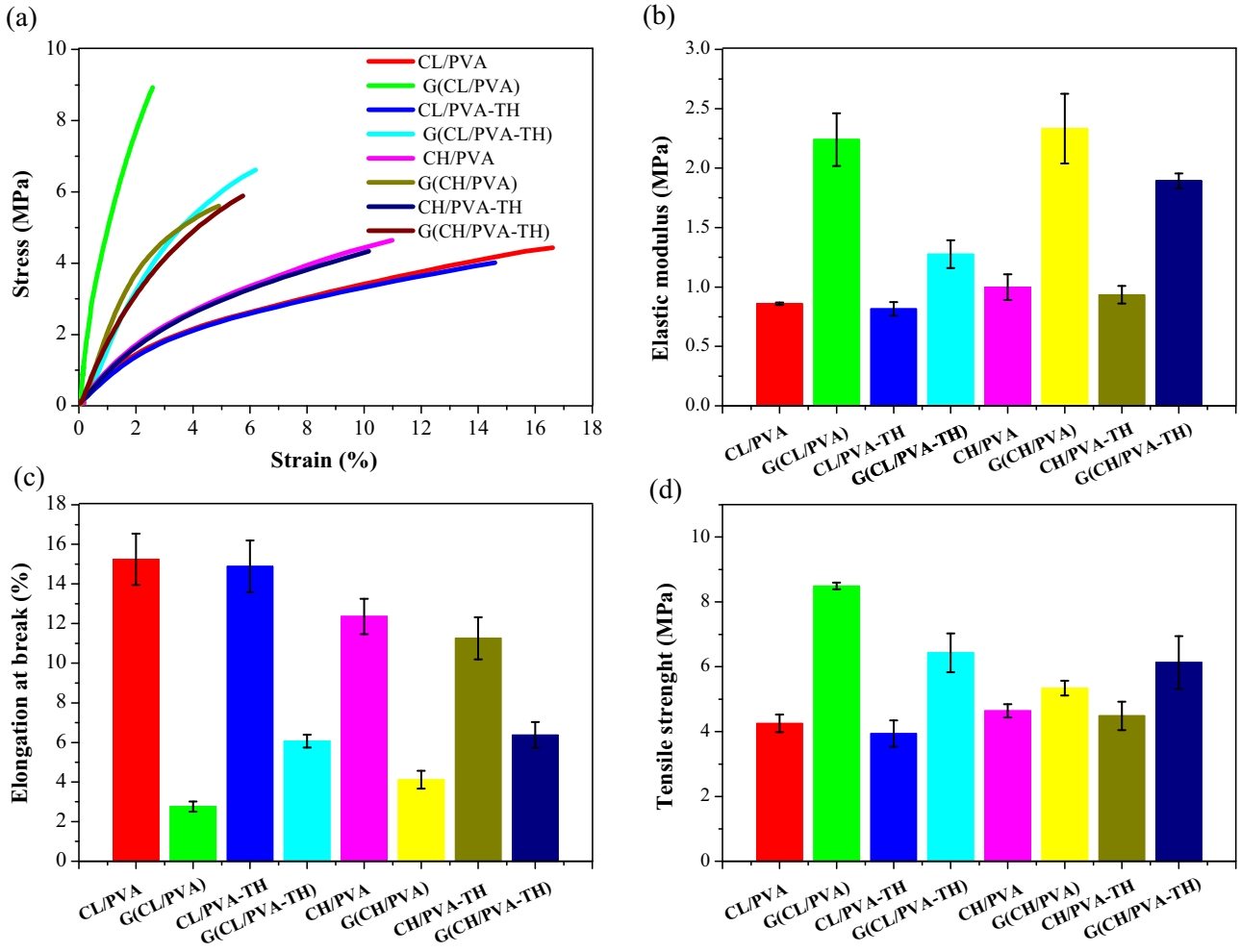

Fig. 7. Stress-strain curves for non-cross-linked (CL/PVA, CL/PVA-TH, CH/PVA, CH/PVA-TH) and cross-linked (G(CL/PVA), G(CL/PVA-TH), G(CH/PVA), G(CH/PVA-TH)) nonwovens and calculated elastic modulus (b), elongation at break (c) and tensile strength (d).

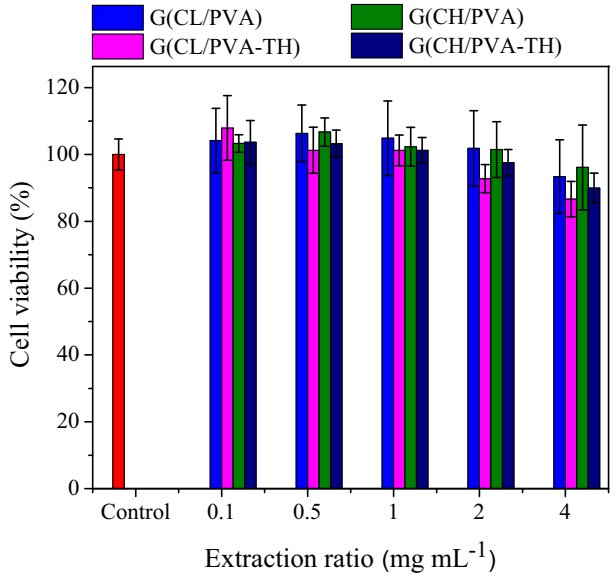

Fig. 8. Dependence of the HDFn cell viability on the cross-linked nonwovens' composition (G(CL/PVA), G(CL/PVA-TH), G(CH/PVA), G(CH/PVA-TH)) and extraction ratios.

to the faster release of TH associated to a dissolution mechanism [67,68]. Similar results were reported by Qin et al. [69], which incorporated aspirin into chitosan-based nanofibers prepared by electrospinning demonstrating that the drug was completely released after 60 s due to fast dissolution of polymeric matrix.

On the other hand, the cross-linked nonwovens exhibited a small burst release of TH (≈15%) in the first 3 h followed by a sustained release over a period of 14 days, in the presence and absence of lysozyme (Fig. 6d). The initial burst release can be ascribed to the dissolution of non-cross-linked portion of chitosan in the outer shell and the PVA in the inner core. As previously demonstrated, the crosslinking resulted in decrease of swelling capacity of nonwovens as well as increase of the stability of these materials in aqueous medium, thus decreasing the release rate of TH by diffusion and dissolution of polymeric matrix and consequently promoting a sustained release. This behavior can be also associated to the core-sheath fibers structure, once the genipin-crosslinked-chitosan in the sheath layer serves as a diffusive barrier for the drug in the core layer. Several studies have demonstrated the advantages of core-sheath nanofibers over monolithic nanofibers for bioactive compounds release, including uniform distribution of bioactive agent into the nanofibers, sustained release and protection of the incorporated bioactive compound [23,70–73]. For example, Sultanova et al. [74] compared blended and coaxial electrospun polycaprolactone (PCL)-based nanofibers for hydrophilic

Please cite this article as: D. M. dos Santos, P. A. M. Chagas, I. S. Leite et al., Core-sheath nanostructured chitosan-based nonwovens as a potential drug delivery system for periodontitis treatment, International Journal of Biological Macromolecules, https://doi.org/10.1016/j.ijbiomac.2019.09.124

model drug (ampicillin) encapsulation, and the results showed that the drug release from the coaxial fibers exhibited better sustained-release profiles with a smaller initial burst effect compared to drug released from monolithic electrospun fibers.

Results also reveal that the release profile of TH from cross-linked nonwovens in the presence of lysozyme was highly dependent on the structural characteristics of chitosan, as a higher TH release rate was observed from the nonwovens prepared from the more acetylated chitosan (CL; $\overline{DD}$ = 82%). Indeed, these results are in agreement with the findings from *in vitro* degradability study of nonwovens, which evidenced the increase of stability in aqueous medium in the presence of lysozyme when the more acetylated chitosan (CL) was present in the shell layer. Overall, G (CH/PVA-TH) nonwoven can be considered potentially useful as a platform for local hydrophilic drug delivery in periodontitis treatment, once it presented an initial burst release that can be advantageous in improving the therapeutic effect at the beginning, and the sustained release can hinder the occurrence of new bacterial infection [11,75,76]. These novel sustained drug delivery systems combine the benefits of core-sheath structure and the nontoxic nature, biocompatibility, and biodegradability of chitosan in sheath layer. In addition, it is well-known that chitosan exhibits mucoadhesive property, which is desirable for designing drug delivery systems by increasing the residence time and minimizing the degradation of drug at the absorption site, thus improving the therapeutic efficacy [77–79].

3.8. Mechanical properties

A GTR membrane should have adequate mechanical properties to facilitate handling and application and to support cells related to periodontal regeneration [7]. In this regard, the mechanical properties of coaxial electrospun nonwovens were investigated by tensile tests, and their typical strain-stress curves are presented in Fig. 7a, while the elastic modulus, elongation at break and tensile strength calculated from these curves are summarized in Fig. 7b, c and d, respectively. As can be seen, after crosslinking the elastic modulus and tensile strength increased and the elongation at break decreased, regardless of nonwoven composition. This behavior may be explained by the formation of covalent bonds between genipin and chitosan chains, which limits the mobility of the chain segments and results in a more rigid material. It is worth noting that all cross-linked nonwovens displayed tensile strength values higher than 4 MPa and elongation at break lower than 7%, which may be considered desirable attributes for reducing the risks of material deformation and consequent infiltration of fibroblast cells on periodontal defect, thus favoring the regeneration [7].

3.9. Cytotoxicity assay

The previous discussions clearly demonstrate that genipin-cross-linked nonwovens are potentially useful materials to be used in periodontal regeneration. Regarding the potential biomedical applications of these materials, their biocompatibility should be evaluated. In this study, the cytotoxicity of the cross-linked nonwovens toward neonatal human dermal fibroblast (HDFn) cells was investigated using MTT assay. The fibroblast cells were cultured in different concentrations of the extract solutions of the nonwovens (4, 2, 1, 0.5 and 0.1 mg/mL), and the cytotoxicity was estimated after 24 h (Fig. 8). Cell viability data reveal that regardless of extraction ratio, all nonwovens did not exhibit any toxicity after 24 h in contact with the HDFn cells. In addition, no significant difference in cell viability was noted between the different tested nonwovens (p-value > 0.05). Although further *in vitro* and *in vivo* investigations will be carried out in future experiments, the results indicate that prepared nonwovens exhibited *in vitro* cytocompatibility and hence are prospective candidates for biomedical applications.

3.10. Assessment of antibacterial activity

In the present study, the antimicrobial activity of the cross-linked nonwovens towards a series of bacterial strains obtained from human periodontal subgingival pocket of patients with

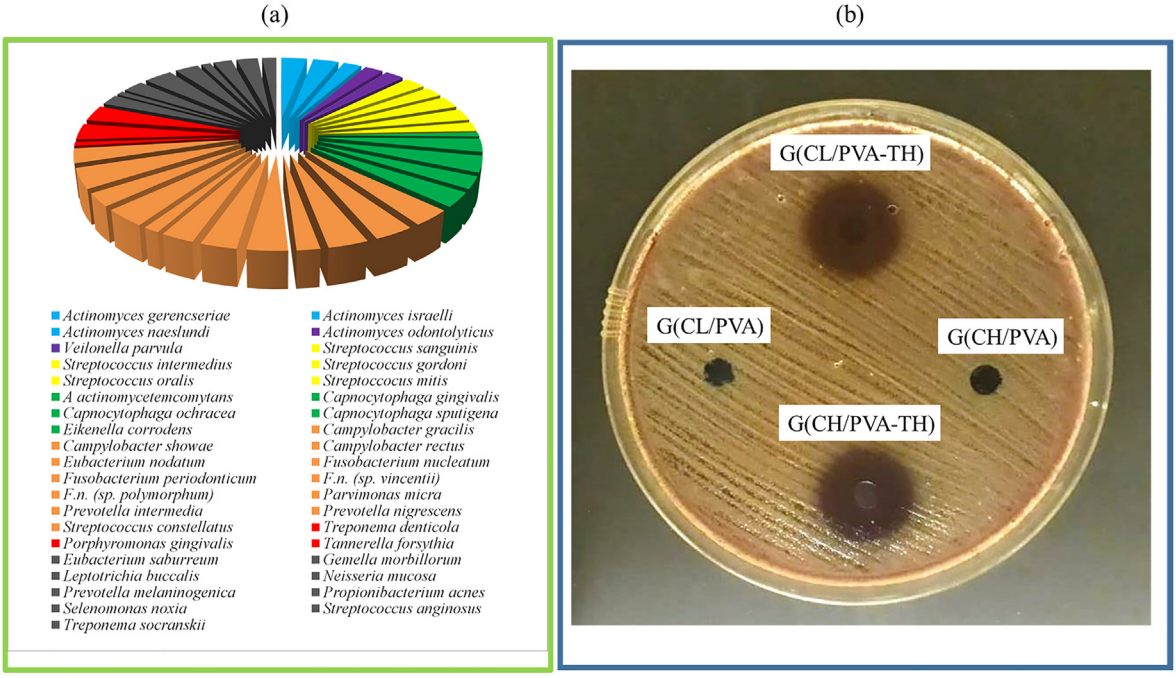

Fig. 9. Bacterial strains present in samples extracted from human periodontal subgingival pocket of patients with chronic periodontitis (a); Antibacterial results for cross-linked nonwovens without TH (G(CL/PVA), G(CH/PVA)) and containing TH (G(CL/PVA-TH), G(CH/PVA-TH)) (b), where the nonwovens were placed on plates previously inoculated with periodontal pathogens.

Please cite this article as: D. M. dos Santos, P. A. M. Chagas, I. S. Leite et al., Core-sheath nanostructured chitosan-based nonwovens as a potential drug delivery system for periodontitis treatment, International Journal of Biological Macromolecules, https://doi.org/10.1016/j.ijbiomac.2019.09.124

chronic periodontitis was evaluated. Periodontal disease involves a highly complex bacterial microbiota, which colonization profile varies qualitatively and quantitatively among individuals. Despite the microbiological variation of each individual, associations between 40 bacterial species present in the subgingival microbiota of individuals with chronic periodontitis have been exhaustively studied and classified by complexes: red, orange, yellow, green and purple [80–82]. Yellow, purple and green complexes members were recognized as early colonizers in periodontal diseases, whereas orange complex precede the colonization of bacteria pertaining to the red complex, which in turn are strongly related to periodontal diseases [83–85].

Results in Fig. 9a reveal that clinical samples displayed a predominance of bacterial species of orange complex (*Fusobacterium nucleatum, Parvimonas micra, Prevotella nigrescens, Prevotella intermedia, Eubacterium nodatum, Campylobacter gracilis, Campylobacter rectus and Campylobacter showae*) and red complex (*Treponema denticola, Tannerella forsythia and Porphyromonas gingivalis*). A homogeneous distribution of bacterial species of green, yellow, purple complexes as well as other component species was also identified.

Fig. 9b shows digital photo of the nonwovens on agar plates in the presence of periodontal pathogens. As can be seen, cross-linked nonwovens without TH incorporation (G(CL/PVA) and G(CH/PVA)) did not present bacterial inhibition zone formation against periodontal pathogens owing to the lack of antibacterial properties of these materials. In contrast, G(GL/PVA-TH) and G(CH/PVA-TH) nonwovens inhibited the bacterial growth, as demonstrated by bacterial inhibition zones for periodontal pathogens (29.0 ± 1.0 mm and 29.0 ± 1.7 mm), thus indicating that the bacterial inhibition effect is solely related to the incorporated antibiotic. It is interesting to note that, although the G(CL/PVA-TH) and G(CH/PVA-TH) nonwovens showed different drug release patterns, the antimicrobial activity of them did not differ significantly (p-value > 0.05) in the antibacterial tests. In addition, results also reveal that the incorporation of TH inside the core of the nanofibers does not compromise the inherent antibacterial activity of this antibiotic. It is worth mentioning that G(GL/PVA-TH) and G(CH/PVA-TH) nonwovens exhibited expressive activity towards a series of bacteria including those of the red and orange complex, which are recognized as pathogens in aggressive and chronic periodontitis [83,86,87], therefore demonstrating their high potential to be used in periodontal treatment.

4. Conclusion

Nonwovens constituted by chitosan/poly (vinyl alcohol) electrospun core-sheath nanofibers were successfully prepared via coaxial electrospinning. The post-electrospinning genipin crosslinking decreased the hydrophilicity, swelling ratio and degradation rate of the nonwovens as well as improved their mechanical properties. As a consequence of higher stability of cross-linked nonwovens in aqueous medium, a sustained release of TH from these structures was observed over 14 days. Moreover, the degradation rate and the release profile of TH in simulated conditions of application in the presence of lysozyme can be controlled by properly selecting the chitosan to be used in the shell layer of nanofibers. Regardless of their compositions, cross-linked nonwovens displayed cytocompatibility. In addition, only structures containing TH exhibited expressive antibacterial activity against a wide range of periodontal pathogens, indicating that the antibacterial activity of TH was not compromised after being loaded into the core-sheath nanofibers and by the crosslinking process. Therefore, the genipin-cross-linked chitosan/poly (vinyl alcohol) electrospun core-sheath nonwovens, especially G(CH/PVA-TH), are very promising as a novel drug delivery system in periodontitis treatment.

Declaration of Competing Interest

The authors declare no conflict of interest.

Acknowledgments

The authors thank the financial support from Fundação de Amparo à Pesquisa do Estado de São Paulo (FAPESP) (grant numbers: 2017/20973-4, 2017/12174-4, 2013/07276-1, 2018/23015-7 and 2018/09088-1) Conselho Nacional de Desenvolvimento Científico e Tecnológico (CNPq), MCTI-SisNano (CNPq/402.287/2013-4), Coordenação de Aperfeiçoamento de Pessoal de Nível Superior – Brasil (CAPES) – Código de Financiamento 001 and Rede Agronano (EMBRAPA) from Brazil.

Appendix A. Supplementary material

Supplementary data to this article can be found online at https://doi.org/10.1016/j.ijbiomac.2019.09.124.

References

[1] S.K. Boda, Y. Almoshari, H. Wang, X. Wang, R.A. Reinhardt, B. Duan, D. Wang, J. Xie, Mineralized nanofiber segments coupled with calcium-binding BMP-2 peptides for alveolar bone regeneration, Acta Biomater. 85 (2019) 282–293, https://doi.org/10.1016/j.actbio.2018.12.051.

[2] H. Shimauchi, E. Nemoto, H. Ishihata, M. Shimomura, Possible functional scaffolds for periodontal regeneration, Jpn. Dent. Sci. Rev. 49 (2013) 118–130, https://doi.org/10.1016/j.jdsr.2013.05.001.

[3] M.M. Hasani-Sadrabadi, P. Sarrion, N. Nakatsuka, T.D. Young, N. Taghdiri, S. Ansari, T. Aghaloo, S. Li, A. Khademhosseini, P.S. Weiss, A. Moshaverinia, Hierarchically Patterned Polydopamine-Containing Membranes for Periodontal Tissue Engineering acsnano.8b09623 ACS Nano. (2019), https://doi.org/10.1021/acsnano.8b09623.

[4] American Academy of Periodontolog, Position Paper: Periodontal Regeneration, J. Periodontol. 76 (2005) 1601–1622, https://doi.org/10.1902/jop.2005.76.9.1601.

[5] S. Soltani Dehnavi, M. Mehdikhani, M. Rafienia, S. Bonakdar, Preparation and in vitro evaluation of polycaprolactone/PEG/bioactive glass nanopowders nanocomposite membranes for GTR/GBR applications, Mater. Sci. Eng. C 90 (2018) 236–247, https://doi.org/10.1016/j.msec.2018.04.065.

[6] M. Andrei, A. Dinischiotu, A.C. Didilescu, D. Ionita, I. Demetrescu, Periodontal materials and cell biology for guided tissue and bone regeneration, Ann. Anat. – Anat. Anzeiger. 216 (2018) 164–169, https://doi.org/10.1016/j.aanat.2017.11.007.

[7] M.C. Bottino, V. Thomas, G. Schmidt, Y.K. Vohra, T.-M.G. Chu, M.J. Kowolik, G.M. Janowski, Recent advances in the development of GTR/GBR membranes for periodontal regeneration—a materials perspective, Dent. Mater. 28 (2012) 703–721, https://doi.org/10.1016/j.dental.2012.04.022.

[8] R.A. Fahmy, G.S. Kotry, O.R. Ramadan, Periodontal regeneration of dehisence defects using a modified perforated collagen membrane. A comparative experimental study, Futur. Dent. J. 4 (2018) 225–230, https://doi.org/10.1016/j.fdj.2018.06.004.

[9] D. Joshi, T. Garg, A.K. Goyal, G. Rath, Advanced drug delivery approaches against periodontitis, Drug Deliv. 23 (2016) 363–377, https://doi.org/10.3109/10717544.2014.935531.

[10] S. Kumar, A.P. Singh, S. Senapati, P. Maiti, Controlling drug delivery using nanosheet-embedded electrospun fibers for efficient tumor treatment, ACS Appl. Bio Mater. 2 (2019) 884–894, https://doi.org/10.1021/acsabm.8b00735.

[11] W. Li, Y. Ding, S. Yu, Q. Yao, A.R. Boccaccini, Multifunctional chitosan-45S5 bioactive glass-poly(3-hydroxybutyrate- *co* -3-hydroxyvalerate) microsphere composite membranes for guided tissue/bone regeneration, ACS Appl. Mater. Interfaces. 7 (2015) 20845–20854, https://doi.org/10.1021/acsami.5b06128.

[12] X. Wang, B. Ding, B. Li, Biomimetic electrospun nanofibrous structures for tissue engineering, Mater. Today. 16 (2013) 229–241, https://doi.org/10.1016/j.mattod.2013.06.005.

[13] C.T. Kenry, Lim, Nanofiber technology: current status and emerging developments, Prog. Polym. Sci. 70 (2017) 1–17, https://doi.org/10.1016/j.progpolymsci.2017.03.002.

[14] J. Ding, J. Zhang, J. Li, D. Li, C. Xiao, H. Xiao, H. Yang, X. Zhuang, X. Chen, Electrospun polymer biomaterials, Prog. Polym. Sci. 90 (2019) 1–34, https://doi.org/10.1016/j.progpolymsci.2019.01.002.

[15] R. Schneider, L.A. Mercante, R.S. Andre, H.D.M. Brandão, L.H. Mattoso, D.S. Correa, Biocompatible electrospun nanofibers containing cloxacillin: antibacterial activity and effect of pH on the release profile, React. Funct.

Polym. 132 (2018) 26–35, https://doi.org/10.1016/j.reactfunctpolym.2018.09.001.
[16] D.A. Locilento, L.A. Mercante, R.S. Andre, L.H. Mattoso, G.L. Luna, P. Brassolatti, F.D.F. Anibal, D.S. Correa, Biocompatible and biodegradable electrospun nanofibrous membranes loaded with grape seed extract for wound dressing application, J. Nanomater. (2019 (2019)) 1–11, https://doi.org/10.1155/2019/2472964.
[17] J. Xue, T. Wu, Y. Dai, Y. Xia, Electrospinning and electrospun nanofibers: methods, materials, and applications, Chem. Rev. 119 (2019) 5298–5415, https://doi.org/10.1021/acs.chemrev.8b00593.
[18] H. Zhou, Z. Shi, X. Wan, H. Fang, D.-G. Yu, X. Chen, P. Liu, The relationships between process parameters and polymeric nanofibers fabricated using a modified coaxial electrospinning, Nanomaterials 9 (2019) 843, https://doi.org/10.3390/nano9060843.
[19] Q. Wang, D.-G. Yu, L.-L. Zhang, X.-K. Liu, Y.-C. Deng, M. Zhao, Electrospun hypromellose-based hydrophilic composites for rapid dissolution of poorly water-soluble drug, Carbohydr. Polym. 174 (2017) 617–625, https://doi.org/10.1016/j.carbpol.2017.06.075.
[20] T. Hai, X. Wan, D.-G. Yu, K. Wang, Y. Yang, Z.-P. Liu, Electrospun lipid-coated medicated nanocomposites for an improved drug sustained-release profile, Mater. Des. 162 (2019) 70–79, https://doi.org/10.1016/j.matdes.2018.11.036.
[21] D.-G. Yu, J.-J. Li, G.R. Williams, M. Zhao, Electrospun amorphous solid dispersions of poorly water-soluble drugs: a review, J. Control. Release 292 (2018) 91–110, https://doi.org/10.1016/j.jconrel.2018.08.016.
[22] Z. Abdali, S. Logsetty, S. Liu, Bacteria-responsive single and core-shell nanofibrous membranes based on polycaprolactone/poly(ethylene succinate) for on-demand release of biocides, ACS Omega 4 (2019) 4063–4070, https://doi.org/10.1021/acsomega.8b03137.
[23] H. Jiang, L. Wang, K. Zhu, Coaxial electrospinning for encapsulation and controlled release of fragile water-soluble bioactive agents, J. Control. Release 193 (2014) 296–303, https://doi.org/10.1016/j.jconrel.2014.04.025.
[24] A. Khalf, S.V. Madihally, Recent advances in multiaxial electrospinning for drug delivery, Eur. J. Pharm. Biopharm. 112 (2017) 1–17, https://doi.org/10.1016/j.ejpb.2016.11.010.
[25] K. Kalantari, A.M. Afifi, H. Jahangirian, T.J. Webster, Biomedical applications of chitosan electrospun nanofibers as a green polymer – review, Carbohydr. Polym. 207 (2019) 588–600, https://doi.org/10.1016/j.carbpol.2018.12.011.
[26] P. Sahariah, M. Másson, Antimicrobial chitosan and chitosan derivatives: a review of the structure-activity relationship, Biomacromolecules 18 (2017) 3846–3868, https://doi.org/10.1021/acs.biomac.7b01058.
[27] R. Shanmuganathan, T.N.J.I. Edison, F. LewisOscar, P. Kumar, S. Shanmugam, A. Pugazhendhi, Chitosan nanopolymers: an overview of drug delivery against cancer, Int. J. Biol. Macromol. 130 (2019) 727–736, https://doi.org/10.1016/j.ijbiomac.2019.02.060.
[28] S.P. Miguel, A.F. Moreira, I.J. Correia, Chitosan based-asymmetric membranes for wound healing: a review, Int. J. Biol. Macromol. 127 (2019) 460–475, https://doi.org/10.1016/j.ijbiomac.2019.01.072.
[29] T. Tamer, M. Collins, K. Valachová, M. Hassan, A. Omer, M. Mohy-Eldin, K. Švík, R. Jurčík, Ľ. Ondruška, C. Biró, A. Albadarin, L. Šoltés, MitoQ loaded chitosan-hyaluronan composite membranes for wound healing, Materials (Basel) 11 (2018) 569, https://doi.org/10.3390/ma11040569.
[30] S.M. Ahsan, M. Thomas, K.K. Reddy, S.G. Sooraparaju, A. Asthana, I. Bhatnagar, Chitosan as biomaterial in drug delivery and tissue engineering, Int. J. Biol. Macromol. 110 (2018) 97–109, https://doi.org/10.1016/j.ijbiomac.2017.08.140.
[31] D.M. dos Santos, A. de Lacerda Bukzem, S.P. Campana-Filho, Response surface methodology applied to the study of the microwave-assisted synthesis of quaternized chitosan, Carbohydr. Polym. 138 (2016) 317–326, https://doi.org/10.1016/j.carbpol.2015.11.056.
[32] M. Rinaudo, Chitin and chitosan: properties and applications, Prog. Polym. Sci. 31 (2006) 603–632, https://doi.org/10.1016/j.progpolymsci.2006.06.001.
[33] T.B. Taketa, D.M. dos Santos, A. Fiamingo, J.M. Vaz, M.M. Beppu, S.P. Campana-Filho, R.E. Cohen, M.F. Rubner, Investigation of the internal chemical composition of chitosan-based LbL films by depth-profiling X-ray photoelectron spectroscopy (XPS) analysis, Langmuir 34 (2018) 1429–1440, https://doi.org/10.1021/acs.langmuir.7b04104.
[34] L. Van der Schueren, I. Steyaert, B. De Schoenmaker, K. De Clerck, Polycaprolactone/chitosan blend nanofibres electrospun from an acetic acid/formic acid solvent system, Carbohydr. Polym. 88 (2012) 1221–1226, https://doi.org/10.1016/j.carbpol.2012.01.085.
[35] S.F. Hosseini, Z. Nahvi, M. Zandi, Antioxidant peptide-loaded electrospun chitosan/poly(vinyl alcohol) nanofibrous mat intended for food biopackaging purposes, Food Hydrocoll. 89 (2019) 637–648, https://doi.org/10.1016/j.foodhyd.2018.11.033.
[36] D. Nataraj, S. Sakkara, M. Meghwal, N. Reddy, Crosslinked chitosan films with controllable properties for commercial applications, Int. J. Biol. Macromol. 120 (2018) 1256–1264, https://doi.org/10.1016/j.ijbiomac.2018.08.187.
[37] R.A.A. Muzzarelli, M. El Mehtedi, C. Bottegoni, A. Gigante, Physical properties imparted by genipin to chitosan for tissue regeneration with human stem cells: a review, Int. J. Biol. Macromol. 93 (2016) 1366–1381, https://doi.org/10.1016/j.ijbiomac.2016.03.075.
[38] A.M. Ramos-de-la-Peña, C.M. Renard, J. Montañez, M. de la Luz Reyes-Vega, J.C. Contreras-Esquivel, A review through recovery, purification and identification of genipin, Phytochem. Rev. 15 (2016) 37–49, https://doi.org/10.1007/s11101-014-9383-z.
[39] A.M. Heimbuck, T.R. Priddy-Arrington, B.J. Sawyer, M.E. Caldorera-Moore, Effects of post-processing methods on chitosan-genipin hydrogel properties, Mater. Sci. Eng. C 98 (2019) 612–618, https://doi.org/10.1016/j.msec.2018.12.119.
[40] A. Fiamingo, S.P. Campana-Filho, Structure, morphology and properties of genipin-crosslinked carboxymethylchitosan porous membranes, Carbohydr. Polym. 143 (2016) 155–163, https://doi.org/10.1016/J.CARBPOL.2016.02.016.
[41] H. Adeli, M.T. Khorasani, M. Parvazinia, Wound dressing based on electrospun PVA/chitosan/starch nanofibrous mats: fabrication, antibacterial and cytocompatibility evaluation and in vitro healing assay, Int. J. Biol. Macromol. 122 (2019) 238–254, https://doi.org/10.1016/j.ijbiomac.2018.10.115.
[42] A.W. Jatoi, H. Ogasawara, I.S. Kim, Q.-Q. Ni, Polyvinyl alcohol nanofiber based three phase wound dressings for sustained wound healing applications, Mater. Lett. 241 (2019) 168–171, https://doi.org/10.1016/j.matlet.2019.01.084.
[43] G. Chaussard, A. Domard, New aspects of the extraction of chitin from squid pens, Biomacromolecules 5 (2004) 559–564, https://doi.org/10.1021/bm034401t.
[44] A. Fiamingo, J.A. de Moura Delezuk, S. Trombotto, L. David, S.P. Campana-Filho, Extensively deacetylated high molecular weight chitosan from the multistep ultrasound-assisted deacetylation of beta-chitin, Ultrason. Sonochem. 32 (2016) 79–85, https://doi.org/10.1016/j.ultsonch.2016.02.021.
[45] A. Hirai, H. Odani, A. Nakajima, Determination of degree of deacetylation of chitosan by 1H NMR spectroscopy, Polym. Bull. 26 (1991) 87–94, https://doi.org/10.1007/BF00299352.
[46] M. Rinaudo, M. Milas, P. Le Dung, Characterization of chitosan. Influence of ionic strength and degree of acetylation on chain expansion, Int. J. Biol. Macromol. 15 (1993) 281–285, https://doi.org/10.1016/0141-8130(93)90027-J.
[47] E. Rojo, M.S. Peresin, W.W. Sampson, I.C. Hoeger, J. Vartiainen, J. Laine, O.J. Rojas, Comprehensive elucidation of the effect of residual lignin on the physical, barrier, mechanical and surface properties of nanocellulose films, Green Chem. 17 (2015) 1853–1866, https://doi.org/10.1039/C4GC02398F.
[48] C.J. Van Oss, M.K. Chaudhury, R.J. Good, Interfacial Lifshitz-van der Waals and polar interactions in macroscopic systems, Chem. Rev. 88 (1988) 927–941, https://doi.org/10.1021/cr00088a006.
[49] D.M. dos Santos, I. Souza Leite, A. de Lacerda Bukzem, R.P. de Oliveira Santos, E. Frollini, N.M. Inada, S.P. Campana-Filho, Nanostructured electrospun nonwovens of poly(ε-caprolactone)/quaternized chitosan for potential biomedical applications, Carbohydr. Polym. 186 (2018), https://doi.org/10.1016/j.carbpol.2018.01.045.
[50] C.J. van Oss, Hydrophobicity of biosurfaces — origin, quantitative determination and interaction energies, Colloids Surf. B Biointerfaces 5 (1995) 91–110, https://doi.org/10.1016/0927-7765(95)01217-7.
[51] ISO10993–5, International Organization for Standardization, Biological Evaluation of Medical Devices Part 5: Tests for In Vitro Cytotoxicity, 5 (2009) 32. https://www.iso.org/standard/36406.html.
[52] A. Neamnark, N. Sanchavanakit, P. Pavasant, T. Bunaprasert, P. Supaphol, R. Rujiravanit, In vitro biocompatibility evaluations of hexanoyl chitosan film, Carbohydr. Polym. 68 (2007) 166–172, https://doi.org/10.1016/j.carbpol.2006.07.024.
[53] C. Clinical and Laboratory Standards Institute (CLSI), Performance Standards for Antimicrobial Susceptibility Testing; Fifteenth Informational Supplement. CLSI/NCCLS document M100-S15, 940 West Valley Road, Suite 1400, Wayne, Pennsylvania 19087 – 1898 USA, 2005.
[54] S.S. Socransky, C. Smith, L. Martin, B.J. Paster, F.E. Dewhirst, A.E. Levin, "Checkerboard" DNA-DNA hybridization, Biotechniques 17 (1994) 788–792 (accessed May 7, 2019) http://www.ncbi.nlm.nih.gov/pubmed/7833043.
[55] M. Pakravan, M.-C. Heuzey, A. Ajji, Core-shell structured PEO-chitosan nanofibers by coaxial electrospinning, Biomacromolecules 13 (2012) 412–421, https://doi.org/10.1021/bm201444v.
[56] N. Bhardwaj, S.C. Kundu, Electrospinning: a fascinating fiber fabrication technique, Biotechnol. Adv. 28 (2010) 325–347, https://doi.org/10.1016/j.biotechadv.2010.01.004.
[57] D.M. dos Santos, A. de Lacerda Bukzem, S.P. Campana-Filho, Response surface methodology applied to the study of the microwave-assisted synthesis of quaternized chitosan, Carbohydr. Polym. 138 (2016) 317–326, https://doi.org/10.1016/j.carbpol.2015.11.056.
[58] J. Brugnerotto, J. Lizardi, F.M. Goycoolea, W. Argüelles-Monal, J. Desbrières, M. Rinaudo, An infrared investigation in relation with chitin and chitosan characterization, Polymer (Guildf). 42 (2001) 3569–3580, https://doi.org/10.1016/S0032-3861(00)00713-8.
[59] N.A. Zubair, N.A. Rahman, H.N. Lim, R.M. Zawawi, Y. Sulaiman, Electrochemical properties of PVA–GO/PEDOT nanofibers prepared using electrospinning and electropolymerization techniques, RSC Adv. 6 (2016) 17720–17727, https://doi.org/10.1039/C5RA21230H.
[60] W. Shao, H. Liu, S. Wang, J. Wu, M. Huang, H. Min, X. Liu, Controlled release and antibacterial activity of tetracycline hydrochloride-loaded bacterial cellulose composite membranes, Carbohydr. Polym. 145 (2016) 114–120, https://doi.org/10.1016/j.carbpol.2016.02.065.
[61] R.A.A. Muzzarelli, Genipin-crosslinked chitosan hydrogels as biomedical and pharmaceutical aids, Carbohydr. Polym. 77 (2009) 1–9, https://doi.org/10.1016/j.carbpol.2009.01.016.

Please cite this article as: D. M. dos Santos, P. A. M. Chagas, I. S. Leite et al., Core-sheath nanostructured chitosan-based nonwovens as a potential drug delivery system for periodontitis treatment, International Journal of Biological Macromolecules, https://doi.org/10.1016/j.ijbiomac.2019.09.124

[62] S.A. Friedman, I.D. Mandel, M.S. Herrera, Lysozyme and lactoferrin quantitation in the crevicular fluid, J. Periodontol. 54 (1983) 347–350, https://doi.org/10.1902/jop.1983.54.6.347.
[63] B. Porstmann, K. Jung, H. Schmechta, U. Evers, M. Pergande, T. Porstmann, H.-J. Kramm, H. Krause, Measurement of lysozyme in human body fluids: comparison of various enzyme immunoassay techniques and their diagnostic application, Clin. Biochem. 22 (1989) 349–355, https://doi.org/10.1016/S0009-9120(89)80031-1.
[64] Z. Liu, B. García-Díaz, B. Catacchio, E. Chiancone, H.J. Vogel, Protecting Gram-negative bacterial cell envelopes from human lysozyme: interactions with Ivy inhibitor proteins from Escherichia coli and Pseudomonas aeruginosa, Biochim. Biophys. Acta – Biomembr. 2015 (1848) 3032–3046, https://doi.org/10.1016/J.BBAMEM.2015.03.024.
[65] K.M. Vårum, H. Kristiansen Holme, M. Izume, B. Torger Stokke, O. Smidsrød, Determination of enzymatic hydrolysis specificity of partially N-acetylated chitosans, Biochim. Biophys. Acta – Gen. Subj. 1291 (1996) 5–15, https://doi.org/10.1016/0304-4165(96)00038-4.
[66] R.J. Nordtveit, K.M. Vårum, O. Smidsrød, Degradation of partially N-acetylated chitosans with hen egg white and human lysozyme, Carbohydr. Polym. 29 (1996) 163–167, https://doi.org/10.1016/0144-8617(96)00003-3.
[67] A. Parmar, S. Sharma, Engineering design and mechanistic mathematical models: standpoint on cutting edge drug delivery, TrAC Trends Anal. Chem. 100 (2018) 15–35, https://doi.org/10.1016/j.trac.2017.12.008.
[68] J. Siepmann, F. Siepmann, Mathematical modeling of drug delivery, Int. J. Pharm. 364 (2008) 328–343, https://doi.org/10.1016/j.ijpharm.2008.09.004.
[69] Z. Qin, X.-W. Jia, Q. Liu, B. Kong, H. Wang, Fast dissolving oral films for drug delivery prepared from chitosan/pullulan electrospinning nanofibers, Int. J. Biol. Macromol. 137 (2019) 224–231, https://doi.org/10.1016/j.ijbiomac.2019.06.224.
[70] J. Wang, M. Windbergs, Controlled dual drug release by coaxial electrospun fibers – impact of the core fluid on drug encapsulation and release, Int. J. Pharm. 556 (2019) 363–371, https://doi.org/10.1016/J.IJPHARM.2018.12.026.
[71] S. Chen, R. Li, X. Li, J. Xie, Electrospinning: an enabling nanotechnology platform for drug delivery and regenerative medicine, Adv. Drug Deliv. Rev. (2018), https://doi.org/10.1016/j.addr.2018.05.001.
[72] P. Wen, Y. Wen, M.-H. Zong, R.J. Linhardt, H. Wu, Encapsulation of bioactive compound in electrospun fibers and its potential application, J. Agric. Food Chem. 65 (2017) 9161–9179, https://doi.org/10.1021/acs.jafc.7b02956.
[73] G. Kabay, C. Demirci, G. Kaleli Can, A.E. Meydan, B.G. Daşan, M. Mutlu, A comparative study of single-needle and coaxial electrospun amyloid-like protein nanofibers to investigate hydrophilic drug release behavior, Int. J. Biol. Macromol. 114 (2018) 989–997, https://doi.org/10.1016/j.ijbiomac.2018.03.182.
[74] Z. Sultanova, G. Kaleli, G. Kabay, M. Mutlu, Controlled release of a hydrophilic drug from coaxially electrospun polycaprolactone nanofibers, Int. J. Pharm. 505 (2016) 133–138, https://doi.org/10.1016/j.ijpharm.2016.03.032.
[75] T.T.T. Nguyen, C. Ghosh, S.-G. Hwang, N. Chanunpanich, J.S. Park, Porous core/sheath composite nanofibers fabricated by coaxial electrospinning as a potential mat for drug release system, Int. J. Pharm. 439 (2012) 296–306, https://doi.org/10.1016/J.IJPHARM.2012.09.019.
[76] P. He, Q. Zhong, Y. Ge, Z. Guo, J. Tian, Y. Zhou, S. Ding, H. Li, C. Zhou, Dual drug loaded coaxial electrospun PLGA/PVP fiber for guided tissue regeneration under control of infection, Mater. Sci. Eng. C 90 (2018) 549–556, https://doi.org/10.1016/J.MSEC.2018.04.014.
[77] J. Meng, V. Agrahari, M.J. Ezoulin, C. Zhang, S.S. Purohit, A. Molteni, D. Dim, N.A. Oyler, B.-B.C. Youan, Tenofovir containing thiolated chitosan core/shell nanofibers: in vitro and in vivo evaluations, Mol. Pharm. 13 (12) (2016) 4129–4140, https://doi.org/10.1021/acs.molpharmaceut.6b00739.
[78] T.M. Ways, W. Lau, V. Khutoryanskiy, Chitosan and its derivatives for application in mucoadhesive drug delivery systems, Polymers (Basel) 10 (2018) 267, https://doi.org/10.3390/polym10030267.
[79] I.A. Sogias, A.C. Williams, V.V. Khutoryanskiy, Why is chitosan mucoadhesive?, Biomacromolecules 9 (2008) 1837–1842, https://doi.org/10.1021/bm800276d.
[80] A.D. Haffajee, R.P. Teles, S.S. Socransky, The effect of periodontal therapy on the composition of the subgingival microbiota, Periodontol. 2000 (42) (2006) 219–258, https://doi.org/10.1111/j.1600-0757.2006.00191.x.
[81] J.J. Kamma, M. Nakou, F.A. Manti, Predominant microflora of severe, moderate and minimal periodontal lesions in young adults with rapidly progressive periodontitis, J. Periodontal Res. 30 (1995) 66–72, https://doi.org/10.1111/j.1600-0765.1995.tb01254.x.
[82] S.S. Socransky, C. Smith, A.D. Haffajee, Subgingival microbial profiles in refractory periodontal disease, J. Clin. Periodontol. 29 (2002) 260–268, https://doi.org/10.1034/j.1600-051x.2002.290313.x.
[83] S. Bathla, Periodontics Revisited, Jaypee Brothers Medical Publishers (P) Ltd., 2012. https://www.doi.org/10.5005/jp/books/11320.
[84] T. Sanghavi, N. Shah, R. Shah, A. Sanghavi, Investigate the correlation between clinical sign and symptoms and the presence of P. gingivalis, T. denticola, and T. forsythia individually or as a "Red complex" by a multiplex PCR method, J. Conserv. Dent. 17 (2014) 555, https://doi.org/10.4103/0972-0707.144604.
[85] A. Contreras, S.M. Moreno, A. Jaramillo, M. Pelaez, A. Duque, J.E. Botero, J. Slots, Periodontal microbiology in Latin America, Periodontol. 2000 (67) (2015) 58–86, https://doi.org/10.1111/prd.12074.
[86] E. Könönen, H.-P. Müller, Microbiology of aggressive periodontitis, Periodontol. 2000 (65) (2014) 46–78, https://doi.org/10.1111/prd.12016.
[87] G.C. Armitage, M.P. Cullinan, Comparison of the clinical features of chronic and aggressive periodontitis, Periodontol. 2000 (53) (2010) 12–27, https://doi.org/10.1111/j.1600-0757.2010.00353.x.

Please cite this article as: D. M. dos Santos, P. A. M. Chagas, I. S. Leite et al., Core-sheath nanostructured chitosan-based nonwovens as a potential drug delivery system for periodontitis treatment, International Journal of Biological Macromolecules, https://doi.org/10.1016/j.ijbiomac.2019.09.124